

Single-cell analysis and sorting using droplet-based microfluidics

Linaz Mazutis^{1,2}, John Gilbert³, W Lloyd Ung¹, David A Weitz¹, Andrew D Griffiths⁴ & John A Heyman^{1,3}

¹School of Engineering and Applied Sciences (SEAS), Harvard University, Cambridge, Massachusetts, USA. ²Institute of Biotechnology, Vilnius University, Vilnius, Lithuania. ³HabSel Inc., Cambridge, Massachusetts, USA. ⁴École Supérieure de Physique et de Chimie Industrielles de la Ville de Paris (ESPCI ParisTech), Centre National de la Recherche Scientifique (CNRS) UMR 7084, Paris, France. Correspondence should be addressed to A.D.G. (andrew.griffiths@espci.fr) or J.A.H. (jheyman@fas.harvard.edu)

Published online 4 April 2013; doi:10.1038/nprot.2013.046

We present a droplet-based microfluidics protocol for high-throughput analysis and sorting of single cells. Compartmentalization of single cells in droplets enables the analysis of proteins released from or secreted by cells, thereby overcoming one of the major limitations of traditional flow cytometry and fluorescence-activated cell sorting. As an example of this approach, we detail a binding assay for detecting antibodies secreted from single mouse hybridoma cells. Secreted antibodies are detected after only 15 min by co-compartmentalizing single mouse hybridoma cells, a fluorescent probe and single beads coated with anti-mouse IgG antibodies in 50-pi droplets. The beads capture the secreted antibodies and, when the captured antibodies bind to the probe, the fluorescence becomes localized on the beads, generating a clearly distinguishable fluorescence signal that enables droplet sorting at ~200 Hz as well as cell enrichment. The microfluidic system described is easily adapted for screening other intracellular, cell-surface or secreted proteins and for quantifying catalytic or regulatory activities. In order to screen ~1 million cells, the microfluidic operations require 2–6 h; the entire process, including preparation of microfluidic devices and mammalian cells, requires 5–7 d.

INTRODUCTION

High-throughput cell-based screens can benefit considerably from the unique liquid-handling capabilities offered by microfluidic systems. This protocol describes the use of two-phase, droplet-based microfluidics systems^{1–3} for high-throughput single-cell analysis and sorting. The basic principle of droplet microfluidic systems is simple: highly monodisperse aqueous droplets flow in an inert carrier oil in microfluidic channels on a chip and each droplet functions as an independent microreactor. Hence, each droplet is the functional equivalent of a well on a microtiter plate. However, the volume of the droplets typically ranges from a few picoliters to a few nanoliters, making the reaction volume roughly a thousand to a million times smaller than in a microtiter plate well (in which the minimum reaction volume is ~1 µl)⁴.

Droplets can be generated and manipulated in a variety of ways. For example, droplets can be split⁵ and new reagents can be added to preformed droplets at defined times in a variety of ways, including by passive droplet fusion^{6,7}, electrocoalescence^{8–10}, picoinjection¹¹ and other techniques^{12,13}. Droplets can be incubated for up to ~1 h in delay lines¹⁴, or incubated for longer times in on-chip^{15,16} or off-chip reservoirs¹⁷. Assays in droplets are typically measured using fluorescence detection techniques^{18,19} and droplets can be selectively sorted using systems based on dielectrophoresis²⁰ or acoustic waves²¹. The sorted droplets are then intentionally broken in order to recover the contents^{22,23}.

Droplet-based microfluidic systems are becoming established as valuable tools for various applications, such as single-cell analysis^{24–34}, complex multistep biological and chemical assays^{17,35–37}, diagnostics^{38–40}, DNA sequencing⁴¹, drug screening^{27,42–44} and directed evolution experiments^{45–47}. Droplets can be generated and manipulated at kHz frequencies³, and compartmentalization of single cells into pico- or nanoliter droplets enables the high-throughput analysis and sorting of millions of individual cells¹. Encapsulated cells remain viable for extended periods of time in droplets²⁵ because of the use of fluorinated carrier oils, which can

dissolve ~20 times more oxygen than water⁴⁸. These oils, being both hydrophobic and lipophobic, are very poor solvents for organic molecules^{49,50} and are thus especially well suited for cell-based assays and biochemical assays.

The small volume of the reaction compartments in droplet-based microfluidic systems provides a number of advantages compared with conventional high-throughput screening systems that use microtiter plates and robotic liquid-handling systems. The benefits of assay miniaturization are clearly demonstrated by a directed evolution experiment to improve the activity of horseradish peroxidase on the surface of individual yeast cells⁴⁵. In total, ~10⁸ individual enzyme reactions were screened in only 10 h, using < 150 µl of reagents—a 1,000-fold increase in speed accompanied by a marked reduction in reagent cost compared with robotic microtiter plate-based screening.

A particular advantage of droplet microfluidics when compared with conventional screening techniques is that droplets provide a unique tool to link genotype with phenotype through compartmentalization⁵¹. Cells and molecules secreted by the cells remain trapped inside the droplets throughout analytical and sorting steps^{45,46,52}. Secreted molecules from single compartmentalized cells quickly reach detectable concentrations because of the small droplet volume^{26,27}, which enables the rapid detection of droplets that contain cells producing molecules of interest. In addition, encapsulated cells can be lysed and intracellular biomolecules assayed^{19,53}. This feature enables biochemical and genetic analyses of cells, as the released DNA or RNA can be amplified in the droplets^{15–17,54–56}. Thus, analysis is highly flexible and not limited to the detection of cell-surface markers, which is typically the case when using classical approaches such as FACS⁵⁷. Although the current throughput of droplet-based microfluidic sorting systems (≤ 2 kHz) is at least an order of magnitude slower than state-of-the-art FACS⁵⁸, the increased flexibility offered by droplet-based microfluidics systems still offers many advantages.

Individual cells can also be compartmentalized in single-phase microfluidic systems. One powerful system pioneered by the Quake research group, and now commercialized by Fluidigm, features sophisticated microfluidic chips composed of multiple valves⁵⁹. The valves can be closed to form compartments of nanoliter volume, which can sequester single cells. These chips have greatly facilitated high-throughput genetic analysis of single cells^{60–62}; however, the maximum number of compartments (and hence single cells) that can be analyzed is currently $\sim 4 \times 10^4$, which limits throughput. Microfluidic devices, containing arrays of microwells of nanoliter volume, have been used to study the proliferation of single hematopoietic stem cells⁶² and to efficiently select single cells that produce antigen-specific antibodies⁶³. These microwell systems, although compatible with a wide variety of assays, require cells of interest to be recovered from the wells using a micropipette, making their use difficult in high-throughput cell-selection applications. In contrast, droplet-based microfluidic systems enable the handling of millions of droplets (and cells) in a single experiment, including sorting at high speed⁴⁵ and recovery of viable cells from the droplets²².

Not all assays are, however, well suited to the droplet format. For example, some biological assays require washing steps, in which reagents from a first reaction must be completely removed before a new set of reagents is introduced. Such heterogeneous assays are difficult to perform inside droplets. Droplet contents can be adjusted through droplet fusion⁷ or by injecting a liquid stream¹¹; however, these procedures do not completely exchange a buffer. The range of readouts for assays in droplet-based microfluidic systems is also currently more restricted than that for conventional microtiter plate assays; most droplet-based microfluidic assays are based on fluorescence⁶⁴, including fluorescence polarization^{65,66} and fluorescence resonance energy transfer (FRET)⁶⁷, although other techniques, such as Raman spectroscopy⁶⁸, have been described, and considerable progress is being made toward the goal of developing highly flexible readouts based on mass spectroscopy³⁵.

Here we present a detailed protocol for using droplet-based microfluidics for high-throughput isolation of individual, antibody-secreting cells from a large excess of nonsecreting cells. The described principles and methods can be adapted for many applications. For example, by screening for antigen binding, the protocol can be extended to facilitate rapid selection of cells secreting target-specific antibody. The assay speed (a single cell in a 50- μ l droplet secretes enough antibody to allow detection in only 15 min) and the high viability of cells in droplets could enable screening of primary cells isolated from human blood, without the need to immortalize the cells. The fluorescence-based binding assay described can also be easily adapted for measuring any secreted molecule for which a fluorescently labeled ligand exists (insulin, cytokines and growth factors among others). In addition, by using fluorogenic substrates or other fluorogenic assays⁶⁹, the protocol is easily adapted for high-throughput screening and directed evolution of enzymes^{45–47}, or for the screening of antibodies and other molecules that inhibit enzyme activity²². This approach can also be used in order to analyze a wide range of cells, including bacteria^{32,52}, yeast⁴⁵, insect³³ and mammalian cells, on the basis of the activities of secreted²⁶, cell-surface^{23,70} or intracellular proteins^{25,27}.

Experimental design

In this protocol, we describe the production and use of microfluidic chips for high-throughput single-cell analysis and screening.

We detail three major steps: (i) microfluidic device (chip) design and fabrication, (ii) cell preparation and encapsulation and (iii) single-cell sorting based on fluorescence. In addition, we detail a useful control protocol to evaluate cell growth in conditions that mimic compartmentalization in droplets, and we describe the use of nonsecreting cells to evaluate the efficiency of the sorting process.

Microfluidic device design and fabrication

We use soft lithography⁷¹ to fabricate microfluidic devices in poly(dimethyl siloxane) (PDMS). The process includes: (i) mask design using computer-aided design (CAD) software, (ii) mask printing, (iii) fabrication of the master, (iv) polymerization of the PDMS using the master as a mold, (v) bonding of the PDMS slabs to a glass substrate and (vi) surface treatment of the microfluidic channels (Fig. 1).

The CAD designs provided as **Supplementary Data** are optimized for cell encapsulation, analysis and sorting, and they should, therefore, enable the production of microfluidic devices without further modifications (Fig. 2). However, it is worth emphasizing some key aspects that will enable users to create their own designs and avoid potential errors. We recommend using a flow-focusing junction⁷² for generating droplets; this geometry produces stable monodisperse droplets at moderate-to-high capillary numbers and lower oil-to-water flow rate ratios than are possible with T-junctions or other geometries^{73–75}. These devices produce highly monodisperse droplets over extended periods of time. In order to prevent clogging of the junction, passive filters should be incorporated upstream of the nozzle with the smallest dimensions equal to or smaller than the nozzle width. Although wider filters can be used, clogging of the microfluidic device becomes more likely with them than with narrower filters.

In order to stabilize droplets against uncontrolled coalescence, the use of surfactants is necessary⁷⁶. These molecules populate the water-oil interface and prevent droplet coalescence. However, diffusion time and interface stabilization are strongly affected by the properties of the surfactants, and it takes several milliseconds for droplets to become stable against coalescence^{7,77}. Therefore, the

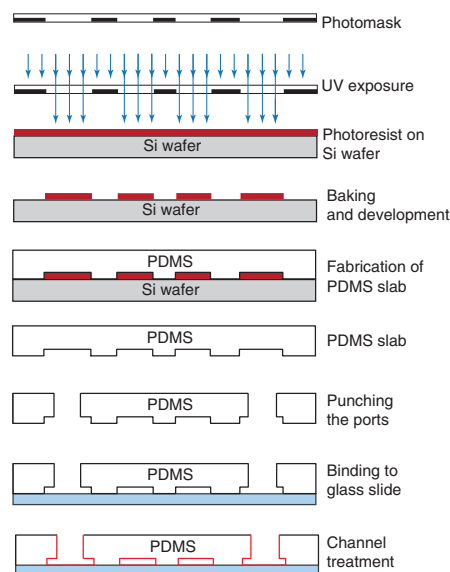
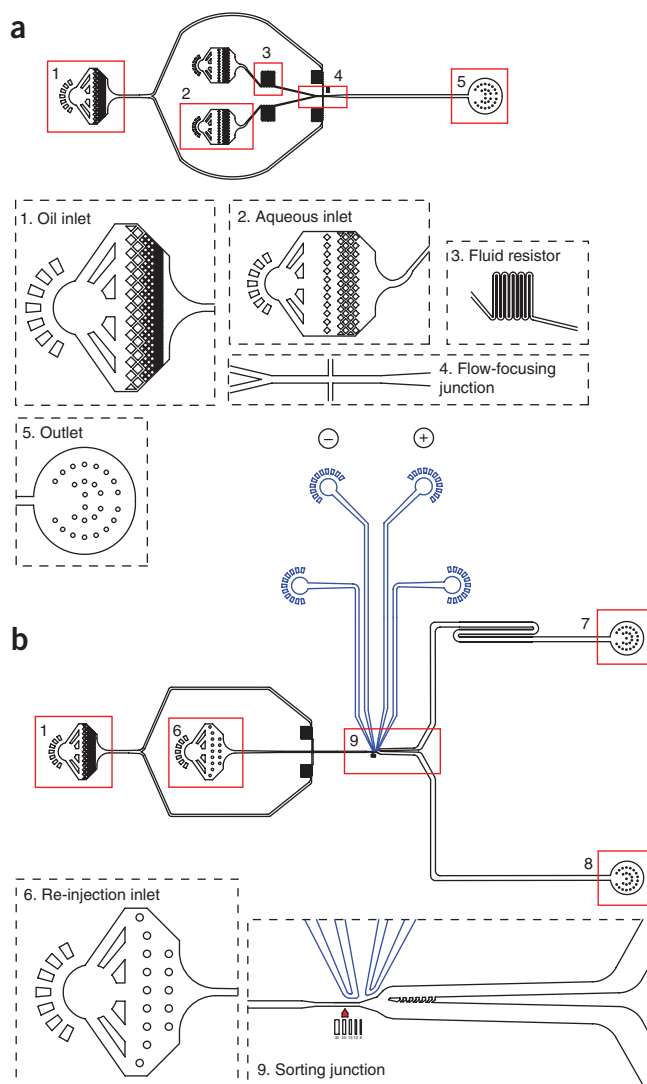


Figure 1 | Schematic of soft lithography.

PROTOCOL

Figure 2 | Design of microfluidic devices. **(a)** Microfluidic device for cell and bead coencapsulation. The device consists of one inlet for the continuous phase (1) and two inlets for different aqueous phases (2). Fluid resistors (3) are placed for both continuous and aqueous phases to dampen fluctuations arising from the mechanical instability of syringe pumps and the elasticity of the PDMS device. Because of laminar flow inside microfluidic channels, the two aqueous streams injected into the device flow side by side and are completely mixed only after they are encapsulated into droplets at the flow-focusing junction (4). Droplets leaving the outlet (5) are collected into a tube or syringe. **(b)** The droplet-sorting device consists of one inlet for the continuous phase (1), one inlet for the re-injected emulsion (6); and two outlets, one for sorted droplets (7) and the other for unsorted droplets (8). After spacing the emulsion droplets with carrier oil, they move down to the sorting junction (9), where individual droplets are sorted on the basis of fluorescence intensity. The edges of microfluidic channels are black, the edges of electrodes are blue, and the red triangle is a mark below the microfluidic channel to indicate where the laser beam should be focused and droplet fluorescence measured. See also **Supplementary Videos 1–3** and **Supplementary Data**.



channel downstream from the nozzle should keep droplets separated from each other for a sufficient period of time to allow droplet stabilization. For the flow rates specified in the protocol, a channel $> 500 \mu\text{m}$ long, corresponding to a droplet residence time of 5–10 ms, is usually sufficient for droplets to stabilize before they reach the expansion, where they start to collide. Lower surfactant concentrations are possible with longer channels⁷⁷.

The surfactant can interact with encapsulated cells or biological molecules. Therefore, in biological assays, biocompatible surfactants must be used^{78,79}, which do not interfere with biochemical reactions or cellular functions. On the basis of our experience and the available literature data^{26,27,70,79}, nonionic surfactants are the best option, in particular those with PEG head groups. When fluorinated carrier oils are used, fluorosurfactants (surfactants with fluorinated tails) are required. Although the range of commercially available fluorosurfactants is much smaller than that of conventional surfactants, biocompatible fluorosurfactants (although expensive) are available from RainDance Technologies, Dolomite and Bio-Rad. Furthermore, instructions in published synthesis protocols^{16,79,80} enable users to produce their own surfactants. We typically use a triblock copolymer containing two perfluoropolyether (PFPE) tails ($M_w \sim 6,000 \text{ gmol}^{-1}$) and a PEG ($M_w \sim 600 \text{ gmol}^{-1}$) head group. The PFPE block is considerably larger than the hydrophilic PEG block, making the surfactant highly soluble in fluorinated oil and nearly insoluble in the aqueous phase. Detailed physicochemical characteristics of such a surfactant have been reported recently⁷.

The use of fluorinated carrier oils drastically reduces the solubility of nonfluorinated compounds^{49,81} in the continuous phase. However, some hydrophobic fluorescent dyes, such as coumarin and resorufin, can solubilize in surfactant micelles⁸² and partition into the continuous phase, resulting in their exchange between the droplets. In order to minimize leakage and exchange of droplet components, we recommend using hydrophilic assay reagents and dyes. For example, fluorescein, rhodamine 110 and coumarin substituted with the hydrophilic methyl sulfonate moiety⁸³ do not leak from droplets over a period of several days, and thus fluorogenic substrates based on these dyes are excellent choices for cell-based assays^{82,84}.

The microfluidic device channel surfaces should be made fluorophilic to ensure reliable and monodisperse droplet production. We detail two simple methods for efficient surface treatment. The first

is based on the commercial water repellent Aquapel and the second on perfluorododecyltrichlorosilane. At the device outlet, droplets can be collected into Eppendorf-type tubes, glass capillaries or syringes, depending on the volume of emulsion. Once collected, the emulsion can be stored at different temperatures ranging from 0°C to 42°C , or higher, if necessary. In order to prevent water loss from the droplet emulsion, it should be stored in a closed system (e.g., syringe or capillary) or in a water-saturated atmosphere.

When experiments require the use of electric fields for applications such as droplet electrocoalescence^{8,27,37}, picoinjection¹¹ or droplet sorting^{23,45,52}, microelectrodes should be prepared by injecting molten solder into preformed channels on the chip, followed by cooling to form solid metallic wires (see Steps 34–39)⁸⁵.

Cell preparation and encapsulation

Cell preparation is another important aspect of the procedure. The key is the prevention of cell lysis and clumping. Adherent cells should be detached from cell culture flasks by gentle methods. For example, PBS supplemented with 2 mM EDTA, rather than standard trypsin-EDTA solutions, may reach that goal and will reduce cell damage. Traces of DNA from lysed cells, which can aggregate and trap cells and cell debris, resulting in device clogging, can be

Box 1 | Predicting the number of cells and beads inside the droplets

The number of cells and beads inside each droplet can be estimated using the Poisson distribution⁹³, in which the probability $P(X=x)$ of finding x cells (or beads) per droplet is given by the equation $P(X=x) = e^{-\lambda}[\lambda^x/x!]$, with λ representing the mean number of cells (or beads) in the volume of each droplet. As a result, droplet occupancy can be tuned by changing the cell density in the aqueous phase. For instance, to encapsulate $\lambda = 0.3$ cells in 50- μ l droplets, cells should be prepared at a density of 6×10^6 cells per ml. Considering that the cell encapsulation process is completely random, this choice of cell density will result in 74.08% of the droplets containing no cells, 22.22% containing a single cell, 3.3% containing two cells and 0.38% containing more than two cells. Following the same approach, we can estimate the number of beads per droplet. If we aim to have a higher average number of beads per droplet, for example, an average of one bead per 50- μ l droplet ($\lambda = 1.0$), we need to prepare a mixture containing $\sim 5 \times 10^7$ beads per ml. Assuming that the rates of encapsulation of cells and beads are mutually independent, the probability of co-encapsulation of x_1 cells and x_2 beads in a single droplet is equal to

$$P(X_1 = x_1, X_2 = x_2) = \frac{e^{-\lambda_1} \lambda_1^{x_1}}{x_1!} \times \frac{e^{-\lambda_2} \lambda_2^{x_2}}{x_2!}$$

where λ_1 is the mean number of cells per droplet and λ_2 the mean number of beads per droplet. If the mean number of cells per droplet is $\lambda_1 = 0.3$ and the mean number of beads per droplet is $\lambda_2 = 1.0$, then the coencapsulation efficiency is $P(X_1 \geq 1 \cdot X_2 \geq 1) = (1 - e^{-\lambda_1})(1 - e^{-\lambda_2}) = 0.259 \times 0.632 = 0.164$, which means that 16.4% of droplets will contain at least one bead and one cell.

effectively removed by DNase I. However, DNase use prevents the amplification of cellular DNA in later steps. Therefore, handling and washing of cells with physiological buffers or growth media in a careful and gentle manner is the most common way to prepare clean cell suspensions. Some applications may require cell prestaining before encapsulation. Various cellular dyes are available commercially for that task. We found that Molecular Probes CellTracker fluorescent probes work efficiently, as they show low background noise and do not leak from cells over a period of a few hours, although this behavior may be cell type-dependent.

Cell encapsulation is performed so that the majority of droplets contain no more than one cell (Box 1, Fig. 3 and Supplementary Video 1). Although this protocol results in the formation of some empty droplets, throughput remains high compared with the rate of conventional microtiter plate-based techniques, in which analysis is performed at ~ 1 cell per s (1 Hz) (ref. 4). Alternative encapsulation techniques based on Dean-coupled inertial ordering^{86,87} can be exploited in order to increase the fraction of droplets containing single cells to $\sim 80\%$ (ref. 88), thus increasing the throughput. However, these techniques have been used only for homogenous cell mixtures (or particles) and therefore require further development.

Typically, cell encapsulation requires up to 1 h, and, because cells and growth medium have different densities (1.1 g ml^{-1} (ref. 87) and 1.0 g ml^{-1} , respectively), cell sedimentation can occur and decrease encapsulation efficiency. To prevent sedimentation, a density-matching solution, such as OptiPrep (iodixanol)⁸⁹, can be added to the growth medium in order to increase its density so that it matches that of the cells. Proper density matching prevents sedimentation and clumping, enabling encapsulation efficiency of beads and cells to remain nearly constant over periods of up to 2 h, without adverse cytotoxic effects^{90,91}. An alternative method for preventing cell sedimentation and aggregation is to place a mini stir bar in the cell suspension syringe^{27,92}. However, cells might be damaged during the mixing process and cells flowing from the syringe into the microfluidic chip must travel through the tubing, where sedimentation can also occur. For these reasons, we prefer to use density-matching solutions to prevent cell sedimentation in

the tubing and other parts of the system. After the encapsulation process, droplets containing cells can be stored at 37 °C in a 5% CO₂ atmosphere in a humidified incubator, before further analysis or sorting.

Droplet sorting based on fluorescence

Fluorescence-activated droplet sorting requires specially designed microfluidic devices, which enable the efficient recovery of the desired droplets for further processing. The microfluidic device comprises a re-injection inlet that introduces droplets and an oil inlet that spaces them. The channels from these inlets intersect at the spacing junction (Supplementary Video 2), which is followed by a Y-shaped junction where droplets are actively sorted (Supplementary Video 3) via dielectrophoresis. Separation is based on the electric force that results from the interaction between a nonuniform, applied electric field and the dipole it induces in the droplet. Once a droplet passes a point at which it is irradiated by a laser and the resulting fluorescence is recorded, the sorting electric field is turned on only if the droplet has a fluorescence intensity above a preselected threshold. This field results in a dielectrophoretic force that attracts droplets toward the region of high

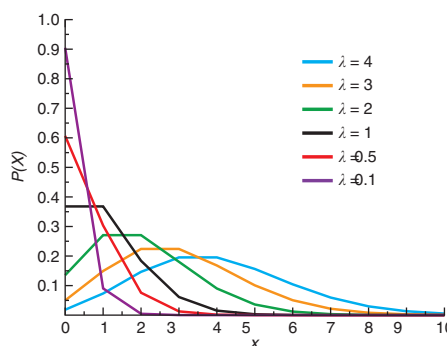


Figure 3 | Probability $P(X=x)$ of finding x number of entities (cell, bead, etc.) at different λ values.

PROTOCOL

field gradient in a manner that depends on the field frequency and the polarizabilities of the droplets and the medium. As the dielectric permittivity of aqueous droplets ($\epsilon \sim 80$) is much higher than that of fluorinated oil ($\epsilon \sim 2$), a positive dielectrophoretic force pulls the droplet toward the high electric gradient region of the device and diverts it into a collection channel. By switching the electrodes on and off, individual droplets can be sorted at frequencies of up to a few kHz (refs. 20,23,45,52). The sorting junction is designed so that the collection channel has 1.2–1.5 times higher fluidic resistance than the waste channel. This difference ensures that, with no applied electric field, all droplets flow into the waste channel. The sharp edges of the electrodes generate the largest field gradients and forces on the droplets²⁰. However, an excessive localized field gradient around the electrode can deform and break droplets passing through the sorting junction. To avoid these high field gradients, the channel immediately upstream of the sorting junction should be wider than the diameter of a droplet and the applied alternating current (AC) voltage across the electrodes should be minimized to the lowest value that results in droplet sorting (typically ~ 1.0 kV peak-to-peak amplitude). The spacing between the droplets is also an important factor affecting sorting efficiency⁵². Two successive droplets moving close to each other can collide at the sorting junction forcing one of the droplets to flow into the collection channel. When correctly spaced with carrier oil such that the distance between two droplets is more than 10 times the size of a droplet, the error rate becomes negligible. During re-injection, a small fraction of droplets can experience uncontrolled coalescence; however, such droplets can be distinguished by their size, and by gating on droplet size (in addition to fluorescence) such droplets are not sorted.

Developing droplet-based microfluidic systems for selecting antibody-secreting cells is a very desirable research goal. Droplet-based fluorogenic assays have been very effective in screens for enzymatic activity, but they have been difficult to adapt to the screening of binding activity. Assays such as ELISA, which are routinely used to screen for antibody binding in microtiter plates, require washing steps and are difficult to implement in droplet-based microfluidic

systems. Here we describe a novel assay to screen for cells secreting antibody in 50- μ l droplets. We illustrate the implementation of the protocol on a mixture of 9E10 cells (mouse hybridoma cells that secrete IgG antibodies against human c-MYC protein) and K562 cells (human chronic myelogenous leukemia cells that do not produce antibodies), with the latter serving as a negative control. The binding assay requires no washing step and is based on the concentration of fluorescence signal on a bead coencapsulated with each cell. In this sandwich assay, the secreted antibodies are captured on the bead surface and detected using a fluorescently labeled secondary antibody. As a result of this interaction, the fluorophore in the droplet becomes concentrated on the bead, thereby generating a clearly distinguishable signal (Figs. 4 and 5). Finally, droplets containing fluorescent beads and coencapsulated cells are selected using a microfluidic sorter. We chose a relatively large droplet size (50 μ l) to improve cell viability and coencapsulation rate. Because of the large droplet size, the throughput of the sorting step in this protocol is 5–10 times lower than that in previous reports^{45,46,52}. This decrease in throughput derives mainly from the fact that larger droplets are more likely to break apart if they impact the sorting junction at high speeds, meaning that more consistent results are obtained by operating at lower sorting rates. However, as the throughput of microfluidic sorting is inversely proportional to the size of the droplets, for applications that do not require large droplets, the sorting rate can be increased above 1 kHz. Overall, the microfluidic system described in this protocol should be easily adapted to screen single cells for other binding interactions, as well as for catalytic or regulatory activities.

The ELISA-type sandwich assay detailed in the **Supplementary Note** is a useful control experiment for testing cell viability and secretory activity of antibody-secreting cells in conditions that mimic compartmentalization in droplets (i.e., at high concentration and in the presence of OptiPrep). We also used this control assay to confirm that antibody is secreted from cells and is not simply leaking from the cells owing to incubation in the presence of OptiPrep. In these experiments, we cultured cells in growth

Figure 4 | Principle of experimental design. Two types of cells (orange and gray ellipses) are introduced together as a cell suspension into a microfluidic device together with a bead suspension. One cell type produces mouse antibodies (gray) and the other does not (orange), with the latter being in 10-fold excess. The bead suspension contains green fluorescent-labeled goat detection antibodies (green) and streptavidin beads coated with goat anti-mouse-Fc capture antibodies (magenta). Because of laminar flow, the two suspensions are only mixed inside the droplets, which are created by flow focusing with fluorinated oil containing fluorosurfactant and then collected off-chip at 4 °C. After incubation for 15 min at 37 °C and 5% CO₂, those beads that are coencapsulated with an antibody-producing cell become highly fluorescent, due to the capture of secreted antibodies on the bead by the anti-mouse Fc antibody and binding of the green fluorescence detection antibodies to the captured antibodies in a sandwich assay. The emulsion is then introduced into a second microfluidic device and droplets containing green fluorescent beads are sorted using a fluorescence-activated droplet sorter. Hence, droplets containing no bead, no cell, a cell which does not secrete antibody, or an antibody-producing cell but no bead are discarded (no green fluorescent bead is present), whereas droplets containing an antibody-producing cell and a bead (which becomes fluorescent) are collected. The three micrographs show coencapsulation of cells with beads (left), droplet re-injection after incubation off-chip (middle) and droplet sorting (right). Ab, antibody.

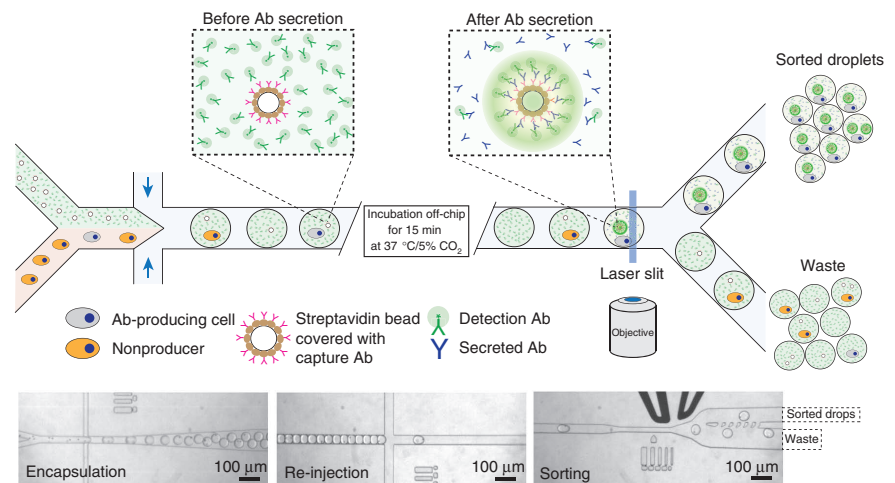
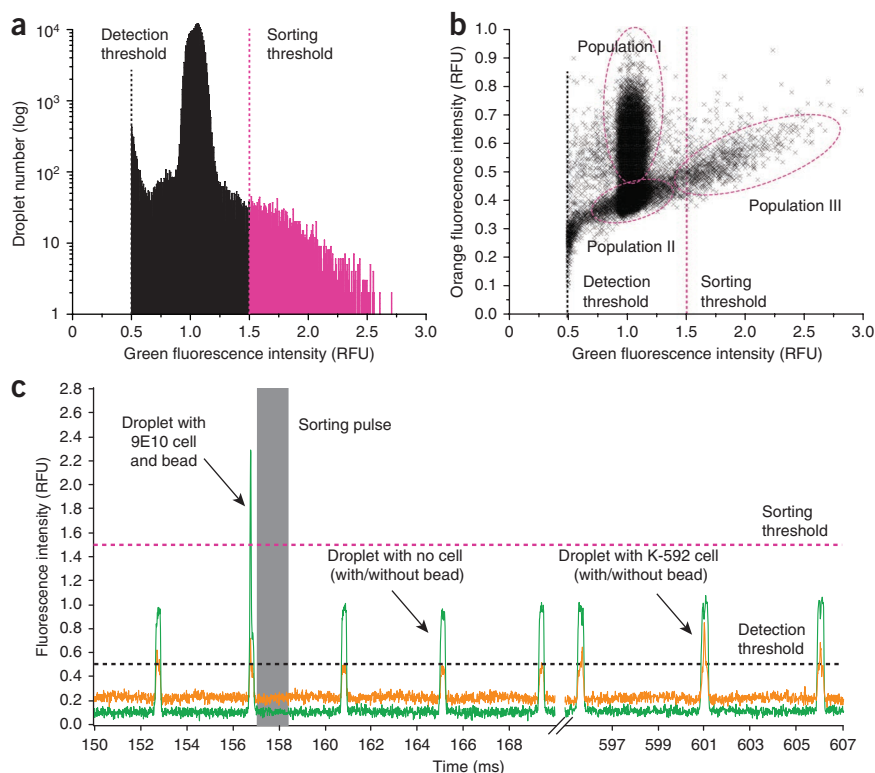


Figure 5 | Fluorescence analysis and sorting of droplets. A mixture of two types of cells, 9E10 (mouse hybridoma cells that secrete anti-MYC antibody) and K562 (human leukemia cells that do not produce antibodies) were coencapsulated with capture beads into 50 pl droplets. K562 cells, which were in 10-fold excess with respect to 9E10 cells, were prestained with orange CMRA dye before encapsulation making them distinguishable from 9E10 cells. **(a)** Histogram showing the distribution of droplet green fluorescence intensity. The detection threshold (black dashed line) was set at 0.5 relative fluorescence units (RFU) to detect all the droplets passing through the detection point. Fluorescent droplets passing the sorting threshold (magenta dashed line) were sorted and collected off-chip into a tube. The droplet population having green fluorescence at ~1.0 RFU corresponds to droplets having cells that do not produce antibodies, as well as droplets with no cells. **(b)** 2D scatter plot of droplet fluorescence intensity during the sorting process. Purple-dashed ellipses indicate different droplet populations. Population I contains droplets with a K562 cell (with or without a bead). Population II contains droplets with a 9E10 cell and no bead, and droplets lacking any cell (with or without a bead). Population III contains droplets with a 9E10 cell and a bead. Droplets containing K562 and 9E10 cells coencapsulated with a bead fall into the region between ~0.5 and 1.0 orange RFU and ~1.2 and 3.0 green RFU. The slight tilt observed in green fluorescence is due to the small fraction of green fluorescence being detected by the orange PMT. **(c)** Fluorescence intensity of individual droplets during microfluidic analysis and sorting. See also **Supplementary Video 3**.



medium supplemented with OptiPrep and detected antibody in the supernatant from cells cultured at 37 °C but not in the supernatant from cells cultured at 4 °C. If cells were lysing, antibody would have been found in the supernatant of cells cultured at 4 °C as well. When necessary, the sandwich assay can be used to efficiently test a variety of cell culture media and conditions, simplifying the identification of conditions that are appropriate for cell growth in droplets. In addition, the PROCEDURE section (Steps 54–62) details the use of cells that do not secrete antibody,

in this case K562 cells stained with the live dye CellTracker Orange CMRA, to confirm sorting results. The fluorescence of the cells enables the user to determine, by fluorescence microscopy, if non-secreting cells are sorted in error. These imaging experiments also enable the user to measure the actual enrichment, independent of that reported by the sorting instrument. In addition, the fact that CMRA does not leak from the K562 cells indicates that the cells remain viable over the course of the entire encapsulation and sorting process.

MATERIALS

REAGENTS

Chemistry

- SU-8 photoresist (MicroChem, SU-8 2025 or 3025) **! CAUTION** SU-8 photoresist is highly flammable and highly toxic. Avoid direct contact with this reagent. Use it only in a well-ventilated area, in a fume hood or with respiratory protection.
- Propylene glycol monomethyl ether acetate (PGMEA; Sigma-Aldrich, cat. no. 537543) **! CAUTION** This solvent is highly flammable. Use a fume hood and wear appropriate protective clothing and equipment when handling it. After use, dispose of it as hazardous waste.
- poly(dimethyl siloxane) (PDMS) and curing agent (Dow Corning, Sylgard 184)
- Acetone (Sigma-Aldrich, cat. no. 534064) **! CAUTION** This solvent is highly flammable. Work in a fume hood and wear appropriate protective clothing and equipment when handling it.
- Ethanol (Sigma-Aldrich, cat. no. 459836) **! CAUTION** This material is highly flammable.

- Isopropanol (Sigma-Aldrich, cat. no. 278475) **! CAUTION** This material is highly flammable.
- Methanol (Sigma-Aldrich, cat. no. 322415) **! CAUTION** This liquid is highly flammable and toxic. Use a fume hood and wear appropriate protective clothing and equipment when handling it.
- Aquapel (Aquapel, cat. no. 47100) **! CAUTION** This material is highly toxic and moisture sensitive. Work in a fume hood and wear appropriate protective clothing and equipment when handling it.
- 1H,1H,2H,2H-Perfluorododecyltrichlorosilane (Sigma-Aldrich, cat. no. 729965) **! CAUTION** This material is highly toxic and moisture sensitive. Use only in a fume hood and wear appropriate protective clothing and equipment when handling it.
- FC-40 oil (3M, cat. no. 98-0212-3550-6) **! CAUTION** Avoid direct contact with this liquid, as it may cause respiratory, skin and eye irritation. Wear appropriate laboratory clothing and equipment.
- HFE-7500 (3M, cat. no. 98-0212-2928-5) **! CAUTION** Avoid direct contact with this liquid, as it may cause respiratory, skin and eye irritation.

PROTOCOL

Wear appropriate laboratory clothing and equipment when handling it.

- Fluorinated surfactant synthesized as described in refs. 16,79,80 or purchased (e.g., RainDance Technologies, Dolomite Pico Surf).
- 1H,1H,2H,2H-perfluoro-1-octanol (PFO; Sigma-Aldrich, cat. no. 370533)
! CAUTION Wear appropriate laboratory clothing and equipment and avoid contact with skin when handling this reagent. Use it only in a fume hood.
- PMSF (Sigma-Aldrich, cat. no. P7626) **! CAUTION** This reagent is highly toxic and can cause severe skin or eye damage. Wear appropriate laboratory clothing and equipment when handling it.
- Pressurized nitrogen
- Pressurized oxygen (for the oxygen plasma cleaner)

Molecular biology

- 9E10 mouse hybridoma cell line (ATCC, cat. no. CRL-1729)
- K562 human chronic myelogenous leukemia cell line (ATCC, cat. no. CCL-243)
- DMEM (Mediatech, cat. no. 10-013-CV)
- FBS (Life Technologies, cat. no. 10313-039)
- Penicillin-streptomycin (Life Technologies, cat. no. 15140-122)
- Streptavidin-coated beads, 6 μm (Spherotech, cat. no. SVP-60-5)
- Capture antibody: biotinylated whole goat IgG directed against the Fc fragment of mouse IgG (Jackson ImmunoResearch Laboratories, cat. no. 115-065-008)
- Detection antibody: whole goat IgG directed against the F(ab)2 fragment of mouse IgG, labeled with dylight 488 (Jackson ImmunoResearch Laboratories, cat. no. 115-485-006)
- Purified anti-MYC mouse monoclonal antibody (Covance, cat. no. MMS-150P)
- Orange CMRA (9'-(4-(and 5)-chloromethyl-2-carboxyphenyl)-7'-chloro-6'-oxo-1,2,2,4-tetramethyl-1,2-dihydropyrido[2',3'-6]xanthene; Invitrogen, CellTracker Orange CMRA ex/em 548/576 nm, cat. no. C34551)
- Magnesium chloride hexahydrate ($\text{MgCl}_2 \cdot 6\text{H}_2\text{O}$; Sigma-Aldrich, cat. no. M-2670)
- PBS (Lifetech, cat. no. 10010-023)
- DNase I (Fermentas, cat. no. EN0521)
- Trypsin (Sigma-Aldrich, cat. no. T4549)
- OptiPrep density gradient medium (Sigma-Aldrich, cat. no. D1556)
- Tween 20 (Sigma-Aldrich, cat. no. P9416)
- Triton X-100 (Sigma-Aldrich, cat. no. T8787)
- Milli-Q ultrapurified water

EQUIPMENT

- Droplet screening instrument (refer to the description in Equipment Setup and alignment procedure in **Box 2**)
- Data acquisition card (PCIe-7842R; National Instruments, cat. no. 781101-01)
- Bright-field inverted microscope (e.g., Nikon, Olympus, Zeiss, Leica)
- Spin coater (Laurell, model WS-650MZ-23NPP)
- Oxygen plasma cleaner (GaLa Instrumente, Plasma Prep 2)
- UV light source (OAI, model LS30/5)
- Ceramic hot plates (VWR, cat. no. 97042)
- Three syringe pumps (Harvard Apparatus, PHD 2000/2200, cat. no. 702001) or equivalent pumps such as those from KD Scientific, Chemyx, Cetoni, New Era, and so on
- Planetary centrifugal mixer (Thinky, Planetary Centrifugal 'Thinky' mixer, cat. no. ARE-310)
- Open-air shaker (e.g., Thermo Fisher Orbital Roto Mix 8 \times 8 or similar)
- Air blower (Giottos Rocket Air Blower) or canned air duster
- High-voltage amplifier (TREK, cat. no. 623B or 2210)
- Oven (65 $^{\circ}\text{C}$)
- Cell culture incubator
- Benchtop centrifuge
- Vortex mixer
- Stereomicroscope
- Biosafety cabinet
- Vacuum desiccator
- Digital multimeter
- Laser safety goggles (Thorlabs, cat. no. LG3 Orange Lens)
- LabVIEW software (LabVIEW Core and LabVIEW field-programmable gate array (FPGA); National Instruments)
- AutoCAD software (Autodesk)
- Silicon wafers (3-inch diameter, Type-P, 1S polished; University Wafer, cat. no. S3P01SP)

- Indium tin oxide (ITO) glass (50 \times 75 \times 0.7 mm; Delta Technologies, cat. no. CG-81IN-S207)
- Cover glass (24 \times 60 mm, No. 1.5; Corning, cat. no. 2980-246)
- Glass slides (75 \times 50 mm; Corning, cat. no. 2947-75X50)
- Low-melting-temperature solder wire (composition 32.5 Bi, 16.5 Sn, diameter 0.020 mm; The Indium Corporation of America, cat. no. wirebn-53307)
- Cutting mat (6 \times 8 inches; Ted Pella, Harris cutting mat, cat. no. 15097)
- Biopsy punches (0.5 and 0.75 mm diameter; Ted Pella, Harris Uni-Core, cat. no. 15071 and 15072)
- Hamilton gas-tight syringe, 2.5 and 5 ml (Hamilton, cat. no. 201300)
- Millipore filter, 0.22 μm (PVDF and polyethersulfonate type)
- Needles (23 gauge and 27.5 gauge; Terumo Neolus, cat. no. NN2325R)
- Sterile 1 ml syringes (Braun Omnifix, cat. no. 9204512)
- PTFE microtubing (0.56 \times 1.07 mm; Fisher Scientific, cat. no. W39241)
- PE-2 tubing (Intramedic)
- Hemocytometer (Hausser Scientific, cat. no. 1490)
- Loctite 352 light cure adhesive glue (Henkel, cat. no. 135412)
- Hollow rectangle glass capillary tubes (0.05 \times 0.5 \times 50 mm; Fiber Optics Center, Vitrocom, cat. no. 5005-050) for droplet observation
- High-binding-capacity streptavidin 96-well plates (Pierce, cat. no. 15503)
- Spin-filter columns (Costar, cat. no. 8162)
- Adjustable 10, 200 and 1,000 μl pipettes and sterile pipette tips
- Pipettes (5, 10, 25 and 50 ml; BD Falcon, cat. no. 357543, 357771, 357550 and 357600)
- Sterile microcentrifuge tubes (0.5 ml and 1.5 ml)
- Sterile conical tubes (15 ml and 50 ml; BD Falcon, cat. no. 352196 and 352070)
- Scalpel (Becton Dickinson, No. 11, cat. no. 371611)
- Diamond pen (VWR, cat. no. 201-0392)
- Petri dishes (100 mm diameter \times 15 mm; BD Falcon, cat. no. 351029)
- Powder-free gloves
- Wafer-handling tweezers
- Sharp tweezers
- Crystallizing dishes (Corning, cat. no. 3140-100)
- Disposable mixing cups
- Frosted Scotch tape
- Aluminum foil

REAGENT SETUP

1% (vol/vol) perfluorododecyltrichlorosilane solution Mix 10 μl of 1H,1H,2H,2H-perfluorododecyltrichlorosilane with 990 μl of HFE-7500 fluorinated oil in a 1.5-ml tube (other fluorinated oils can be used as solvents, but we have not thoroughly tested them). Use this reagent immediately after preparation.

Complete DMEM Mediatech DMEM is supplemented with 10% (vol/vol) FBS and 1% (vol/vol) penicillin-streptomycin. This solution is stable for several weeks at 4 $^{\circ}\text{C}$.

Capture beads We prepare the bead solution at one bead every 50 pl so that the bead occupancy is 0.5 beads per droplet. Approximately 4×10^6 beads are used in a 200- μl aliquot. The streptavidin-conjugated beads must first be coated with biotinylated anti-mouse antibody. The bead-binding capacity is $\sim 4 \times 10^6$ biotin-FITC molecules per bead. We use an excess of biotinylated antibody, 12×10^6 molecules per bead, to coat the beads. Once prepared, beads are stable for several days at 4 $^{\circ}\text{C}$.

DNase solution DNase solution is PBS buffer (1 \times) supplemented with 1 mM MgCl_2 and 25 $\mu\text{g ml}^{-1}$ DNase I. This solution is stable for several days at 4 $^{\circ}\text{C}$.

Wash buffer Prepare 0.05% (vol/vol) Tween 20 in PBS. This buffer is stable for several months at 4 $^{\circ}\text{C}$.

200 mM PMSF in isopropanol Dissolve 200 mM PMSF in isopropanol. This solution is stable for several months at 4 $^{\circ}\text{C}$.

EQUIPMENT SETUP

Droplet screening instrument The optical setup for measuring droplet fluorescence is outlined in **Figure 6**. The expanded laser beam (Melles-Griot 85-BCD 050-115) passes a cylindrical lens of 200-mm focal length (Thorlabs LJ1653RM-A) arranged to focus at the receiving image plane of the microscope objective. We use a Nikon Diaphot cube for a 488-nm laser (Chroma z488rdc-C126912) to route that light to the sample through the microscope objectives. The beam image formed through a $\times 20$ objective is a long narrow slit of 488-nm illumination having full width at half maximum of $\sim 7 \mu\text{m}$ perpendicular to the direction of fluid flow in the microchannel when

Box 2 | Droplet screening instrument optical alignment procedure ● TIMING 1–2 d

Additional materials

- Optics table or bread board
- Optics posts and bases
- Beam-steering mirrors with kinematic mounts (Thorlabs, cat. no. KCB1 and NB1-J10)
- z axis translation mount (Thorlabs, cat. no. SM1Z)
- Rotational mount (Thorlabs, cat. no. SM1V05)
- XY translation mount (Thorlabs, cat. no. LM1XY)
- Dichroic filter mounts (Thorlabs, cat. no. C4W, FFM1, B3C and B6C)
- Cage rods (Thorlabs, cat. no. ER6)
- Lens tube caps (Thorlabs, cat. no. SM1CP2)
- Shutters (Thorlabs, cat. no. SM1SH1)
- PMT-compatible power supply

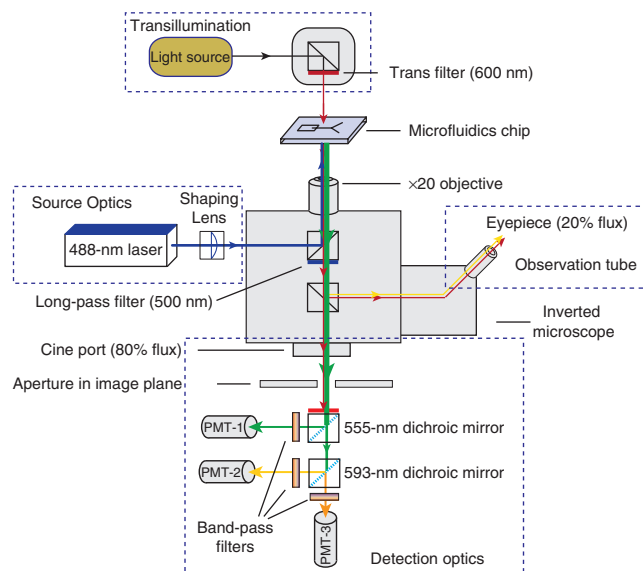
Alignment procedure

! CAUTION In preparation for aligning the system's optical components, please use appropriate laser safety goggles and neutral density filters. Ensure that the long-pass filter is in place at the bottom of the filter cube, to allow the use of the eyepieces. In addition, to prevent stray reflections, remember to use a mechanical shutter to block the beam when adding or removing elements from the laser's beam path.

1. Insert your excitation dichroic into the beam path. It will be aligned by default if you use the appropriate mount provided by the microscope manufacturer.
2. Place the beam expander in front of the laser output.
3. Use mirrors with adjustable tilt mounts to steer the expanded beam through the microscope's epi-illumination port. The laser beam should be visible passing through the microscope objective. If not, remove the objective and make small adjustments to the tilt of each mirror in turn until the beam passes through the center of the empty space in the objective turret. This ensures that the beam will enter the back aperture of the chosen objective. Replace the objective when finished.
4. Use the eyepieces and the microscope reticle, or alternatively a beam target in the focal plane, to center the beam in the field of view.
5. Add the cylindrical lens on a mount with tilt and longitudinal degrees of freedom at a distance such that it focuses light onto the intermediate image plane of the objective. If your microscope objective is infinity corrected, you will need to add a tube lens to the excitation path. When done correctly, a narrow line should appear at the image plane, while the microscope is focused on the device.
6. Use the rotational adjustment to change the angle of the line in the image plane.
7. Adjust the zoom of the cylindrical lens until the line appears sharp when viewed through the eyepieces, while focused on a sample.
8. Remove the filter from the bright-field illumination source. Now the transmitted light can be used to position the detection filters. Place a sample on the microscope and focus it using the eyepieces.
9. A real image of the sample is then projected from the microscope's side port. The adjustable pinhole should be placed at this image plane with an XY-positioning collar.
10. The empty filter cubes should be attached together with cage rods and aligned such that the light passing through the pinhole enters through the center of the entrance port and passes out through the center of the port opposite.
11. Once the cubes are aligned, place the dichroic filters into cubes one at a time, at 45° angles to the incident light, starting with the cube for the shortest wavelength. Adjust the angle of each filter until light of the color chosen for each PMT color is reflected from the dichroic through the center of the PMT-mounting position and the remaining light follows its initial path out through the end of the last detection cube in the array. Repeat this step until all the dichroic filters are in place.
12. (Optional) Once all the dichroic filters have been mounted, it may be necessary to make small adjustments to the position of the entire PMT stack and to positions of individual mirrors. The user should verify that light of the appropriate color from the sample is projected through the center of each PMT port.
13. Replace the filter on the bright-field illumination source.
14. Mount the shutters and band-pass filters in front of each of the PMTs and connect each PMT to the appropriate ports of the filter cube array.
15. Connect the PMTs to a compatible power supply and the data acquisition card. The system should now be able to detect droplet fluorescence.
16. For verification purposes, use a microfluidic channel to flow droplets containing your chosen fluorophores through the laser line. Check that the sample is in focus at the same time that the fluorescence signal on all PMTs is maximized. Follow steps 17–19 to improve the measured signal or when realigning the optical elements.
17. (Optional) To improve the measured signal, it may be necessary to adjust the focus of the laser line, the lateral position and size of the pinhole and the tilt of the individual dichroic filters. This goal can be achieved by making small adjustments and observing their effect on the peak droplet fluorescence measured by the instrument.
18. (Optional) To align the pinhole, center it on the fluorescence signal by closing the aperture tightly and turning the XY adjustments carefully until the signal is maximized.
19. Once centered, open the aperture fully, then close it slowly while observing the measured fluorescence signal until the noise floor stops decreasing and the measured signal starts to fall. Lock the aperture in this position.

PROTOCOL

Figure 6 | Schematic of the optical setup. The fluorescence of each droplet is measured as the droplet flows past an observation constraint (OC) in the microfluidic channel in which the whole droplet is constrained to have a cross-section area of $20 \times 25 \mu\text{m}$ as it passes an optical measurement fiducial mark on the chip. In this OC, a 50- μl droplet will extend to be $\sim 100 \mu\text{m}$ in length. The fluorescence measurement setup uses a 50-mW, 488-nm laser and a Nikon Diaphot epi-illumination microscope. Between the laser and the epi-illumination port of the microscope are 'shaping optics' whose task is to form the beam to a narrow line and present it at the input epi-image plane of the Diaphot's 160-mm tube objectives. A Thorlabs OSL1 visible light illuminator is mounted through a 600-nm long-pass filter to provide optional transillumination to the sample and allow simultaneous trans and epi work if needed. The microscope has a side port, where we place the optics for three PMTs to detect three different colors. The microscope contains an internal prism that we use to send 80% of the light collected by its objectives to the PMTs, whereas 20% is routed to the microscope eyepieces. This 80/20 split enables us to mount a digital high-speed camera in one eyepiece to do simultaneous transmission imaging video and three-color-PMT-based fluorescence measurements.



correctly aligned. Both epi- and trans- images from the sample pass through a 500-nm long-pass filter (Chroma HQ500LP) mounted on the cube to pass light to the microscope's side port or the eyepiece. This long pass filter prevents 488-nm photons from entering the eyepieces and photomultiplier tubes (PMTs). A pinhole aperture is placed in the image plane of the microscope side port and is aligned by direct observation to the location of the laser image on the sample. This aperture should be adjusted as detailed in the alignment procedure (Box 2) to reject background fluorescence emanating from outside the droplet. The pinhole is followed by a set of dichroic mirrors to separate wavelength bands for each of the three PMTs (Hamamatsu H5784-20), the first dichroic is a 555-nm long-pass (Semrock FF555-Di02-25) and the second dichroic is a 593-nm long pass (Semrock FF593-Di02-25). Each PMT is isolated by a band-pass filter to define its color channel: PMT-1 uses a 525-nm/45-nm band-pass (Semrock FF01-525/45-25), PMT-2 uses a 572-nm/28-nm band-pass (Semrock 572/28-25) and PMT-3 uses a 697-nm/75-nm band-pass (Semrock FF01-697/75-25-D). Passive optical elements are all from Thorlabs, Chroma or Semrock. Note that in this protocol, the third PMT is not obligatory; however, some biological applications might require a third optical dye. For example, a third fluorescent dye could be used to indicate cell viability or for optical bar-coding of drug compounds^{27,42}.

Custom LabVIEW data acquisition and control software We use custom LabVIEW 2009 software on a PC with a National Instruments FPGA data

acquisition card (PCIe-7842R) to record droplet fluorescence intensities and trigger the electrodes during sorting. The emitted fluorescence is detected by PMTs (Fig. 6) converted into corresponding signal output voltages, filtered if necessary and recorded by the data acquisition card. These voltages are then processed by the FPGA card to identify droplets according to their fluorescence intensity and size (which is calculated from the residence time in the laser spot and can be used to rule out droplets that have undergone coalescence). These characteristics are used in determining whether each droplet should be sorted. When the PMT voltage exceeds a defined threshold and the droplet size is in the expected range ($\pm 5\%$ of the expected size), the electrodes are activated after a defined delay time that corresponds to the time it takes for a droplet to travel from the detection point to the sorting site in the channel. The frequency and length of electrode activation can also be varied accordingly. The computer's CPU runs the user interface, allowing the operator to preview the data and interact with the instrument. Various parameters, including the thresholds for droplet detection and sorting, the gain of the PMTs and the cutoff frequency of the software noise filters can be tuned for best results. Data are streamed from the FPGA to the CPU, which displays them for the user and writes them to the hard disk, providing a record of each run. The data acquisition rate for the system is 100 kHz. The software can be accessed upon request by academic users through Harvard's SEAS Code Repository (1).

PROCEDURE

Mask design and ordering ● TIMING 1–5 d

1| Use CAD software, such as AutoDesk AutoCAD, to design the pattern printed on a photolithography mask. Well-written tutorials are available online (<http://www.cadtutor.net/tutorials/autocad/index.php>), and sample designs are included in **Supplementary Data**.

2| Order photolithography masks from a photo service company (for instance, FineLine Imaging, CAD/Art Services or Selba). Features in the provided designs should be printed at a minimum of 24,000 d.p.i. to achieve sufficient resolution.

▲ **CRITICAL STEP** When drawing designs, avoid overlays, open polygons, random lines or dots, as companies may charge extra to correct these defects.

Master fabrication ● TIMING ~1 h

3| Choose the SU-8 photoresist with a viscosity appropriate for the desired microfluidic channel thickness. For example, 10–20- μm -deep channels of excellent quality can be effectively produced using SU-8 2010 or 2015. Channels 20–40 μm deep can be produced with SU-8 2015, 2025, 2035. For channels deeper than 50 μm , use SU-8 2050 or higher. Follow the

manufacturer's processing guidelines available online (http://www.microchem.com/Prod-SU8_KMPR.htm). In the rest of the PROCEDURE, we provide instructions for obtaining 25- μm -deep microfluidic channels using SU-8 2025.

4| (Optional) Usually, Si wafers arrive clean; however, if there are traces of organic material on the surface, clean the wafers as follows: immerse the wafer in a crystallizing dish filled with acetone and sonicate it for 2–5 min; transfer the wafer into a glass crystallizing dish filled with methanol and sonicate again for 1–2 min; remove the wafer and rinse it thoroughly with isopropanol; blow the isopropanol off with pressurized nitrogen and heat the wafer in a 200 °C oven for 2–5 min to vaporize any leftover solvent.

5| Line the bowl of the spin coater with aluminum foil; place the wafer into the spin coater and dispense ~3 ml of SU-8 2025 onto the center of the wafer.

▲ CRITICAL STEP Avoid trapping air bubbles in the dispensed SU-8 photoresist, as it can distort the quality of SU-8 structures in the later steps.

6| Engage the vacuum and ramp up the rotational speed (at a rate of 300 r.p.m. s^{-1}) to 500 r.p.m. and spin for 15 s; thereafter, ramp up the rotational speed at the rate of 500 r.p.m. s^{-1} to 3,000 r.p.m. and hold at that speed for 30 s to create a flat resist layer of the desired thickness.

7| Prebake the spin-coated wafer by placing it on a 65 °C hot plate for 1 min.

▲ CRITICAL STEP Ensure that the hot plate is leveled so that the coated layer does not flow and cure unevenly.

8| Bake the wafer at 95 °C for 3 min. Note that overbaking does not reduce the quality of the subsequent steps.

▲ CRITICAL STEP Air bubbles should be removed during the soft baking by gently tapping them with a needle tip.

9| Allow the substrate to cool to room temperature (22–23 °C).

? TROUBLESHOOTING

10| Place the photomask on top of the substrate and expose the wafer according to the specifications in the MicroChem SU-8 data sheet available online (http://www.microchem.com/Prod-SU8_KMPR.htm) and the power of your UV source. We typically use a value of 20 s (exposure energy ~10 mJ cm^{-2}) for a 25- μm layer device.

11| Place the substrate on a 65 °C hot plate for 1 min, and then transfer it to a 95 °C hot plate for 3 min.

12| Place the substrate on a solid surface and let it cool to room temperature for 20–30 s.

? TROUBLESHOOTING

13| Submerge the wafer in PGMEA with the SU-8-coated side up and agitate for development either by putting the container on an orbital shaker and gently agitating for ~4 min or by placing the container in an ultrasonic bath for ~1 min. The orbital shaker provides thorough development of the patterned wafer; the ultrasonic bath develops the wafer faster, but this may result in delamination of the desired features.

! CAUTION PGMEA is highly flammable. Conduct this step rigorously in a fume hood.

? TROUBLESHOOTING

14| By using wafer-handling tweezers, remove the wafer from the crystallizing dish and let the liquid drain. Rinse the wafer with isopropanol.

15| Dry the wafer gently with nitrogen.

▲ CRITICAL STEP The appearance of a whitish residue on the surface of the substrate indicates underdevelopment. If such a whitish residue is observed, repeat Steps 13–15 until no whitish residue remains.

16| (Optional) To improve the adhesion of SU-8 to the substrate and to anneal any cracks formed on the SU-8 surface, you may place the wafer on a 150 °C hot plate (or oven) for 10–30 min. Then slowly cool the substrate to room temperature.

17| Use a stereomicroscope to determine the quality of the developed features. To measure the height of the features, use a profilometer or an ellipsometer.

■ PAUSE POINT At this step, the wafer can be transferred into a plastic Petri dish or stored at room temperature in a dust-free, dry and dark environment before use. It will be stable indefinitely in these conditions.

PROTOCOL

Preparation of the PDMS mold ● TIMING 2–12 h

18| Place the completed master wafer in a plastic 100-mm-diameter Petri dish.

19| Weigh 50 g of PDMS base and 5 g of curing agent (10:1 ratio) and mix well, implementing option A if a planetary centrifugal mixer is not available. If a planetary centrifugal mixer is accessible, implement option B instead.

(A) Mixing by stirring

(i) By using the tines of a plastic fork, stir vigorously until the mixture becomes cloudy and full of air bubbles.

▲ **CRITICAL STEP** Incomplete mixing may affect the homogeneity and mechanical properties of the cured PDMS.

(B) Mixing using a centrifugal mixer

(i) Place the container with the PDMS–curing agent mixture in a planetary centrifugal mixer and centrifuge for 30 s and degas for another 30 s.

▲ **CRITICAL STEP** Be sure to counterbalance the weight of the PDMS in the mixer, or it may get damaged.

20| Pour the PDMS mixture into the Petri dish ~5 mm deep and place the Petri dish in a vacuum desiccator. Release the vacuum periodically to prevent the foam from spilling out of the dish.

21| Degas the PDMS until no bubbles remain attached to the device features and no new bubbles are being formed. Usually 5–10 min is sufficient. If a few bubbles persist, blow gently on the PDMS surface using an air blower or canned air to break the bubbles.

22| Bake the PDMS in a 65 °C oven on a flat, level surface for at least 2 h to cure the PDMS. We have noticed that curing overnight gives better quality PDMS slabs.

■ **PAUSE POINT** After curing, the whole Petri dish can be transferred to room temperature and kept for an unlimited period of time before proceeding to the next step.

23| Cut the PDMS slab with a scalpel and gently peel the PDMS from the silicon wafer.

▲ **CRITICAL STEP** Please note that exerting excessive force will cause the wafer to shatter.

? TROUBLESHOOTING

24| Cover the nonpatterned side of the PDMS slab with frosted Scotch tape, and then place the device on a cutting mat with the channels facing upward.

25| Use a biopsy punch to create holes at each fluid inlet or outlet. Devices with microelectrodes require additional holes, at a different punch diameter, for efficient solder filling.

▲ **CRITICAL STEP** The size of the biopsy punch should be 1.2–1.5 times smaller than the outer diameter of the tubing to be used. We use a 0.75-mm-diameter biopsy punch for PE-2 tubing (Intramedic) or PTFE microtubing with outer diameters of ~1 mm. For microelectrode channels, we use a 0.5-mm-diameter biopsy punch.

? TROUBLESHOOTING

26| Cover the patterned side of the PDMS with frosted Scotch tape so that both sides of the PDMS slab are now covered. Place the device, channel side down, on your work surface. Peel off the Scotch tape from the top side. This will remove most of the debris that results from PDMS hole punching.

27| Remove the Scotch tape from the patterned side and use sharp tweezers to remove any PDMS plugs that remain lodged inside the ports.

28| Flush the PDMS slab holes with isopropanol to ensure complete removal of PDMS debris. Dry under a stream of nitrogen.

29| Select a substrate (50 mm × 75 mm) to seal the PDMS microfluidic device. Use regular glass slides for encapsulating cells within droplets, or use other applications that do not use electrodes; use a glass slide coated with ITO for devices that use microelectrodes. The latter choice permits electrical grounding of the device and reduces undesired electrocoalescence of droplets within the device during sorting. Use an ohmmeter to determine which side is coated with ITO.

30| Place the PDMS slab and the glass slide in the plasma chamber with the channel side facing upward. If ITO glass is used, the ITO coating should be facing downward.

31| Plasma-treat the PDMS slab and the glass slide together. The parameters for plasma treatment depend on the type of machine. For the oxygen plasma cleaner referred in the Materials (GaLa Instrumente, Plasma Prep 2), use the following settings: plasma burst = 10 s, power = 2.5, oxygen level = 8–10.

▲ **CRITICAL STEP** This step must be performed carefully, as it is essential that the binding of the PDMS slab to the glass is strong; otherwise, delamination will occur during microfluidic operations.

? **TROUBLESHOOTING**

32| Remove the PDMS slab and the glass slide from the chamber and bring the plasma-treated faces into contact. Gently press the PDMS so that all parts are sealed to the glass.

? **TROUBLESHOOTING**

33| Place the device in a 65 °C oven for 5–10 min.

■ **PAUSE POINT** The device can be stored in the 65 °C oven for several days. Alternatively, after incubation at 65 °C for 5–10 min, the device can be transferred to room temperature and stored indefinitely in a clean environment before proceeding further.

Microelectrode manufacture ● **TIMING 10–30 min**

34| Place the device on a 90 °C hot plate for 3–5 min.

35| Cut ~5 cm of low-melting-temperature solder wire and use tweezers to insert it into the electrode channels. Solder bends easily; thus it should be held close to the tip. Upon insertion, the solder should melt immediately and start filling the microchannel. Continue pushing the solder into the hole until molten solder emerges from the outlet.

! **CAUTION** Be careful not to burn yourself while working on the hot plate. A face shield should be worn for protection from molten solder spatters.

36| Remove any excess solder using the tweezers to gently scrape solder from the PDMS surface.

37| Insert metal pins into each end of the filled electrode channel. Verify electrical contact using a digital multimeter.

? **TROUBLESHOOTING**

38| Cool the device to room temperature and load it into the oxygen plasma cleaner. Expose the surface to oxygen plasma for 10 s using the following settings: power = 10, oxygen level = 8–10.

39| Apply Loctite 352 around the electrode pins and expose the device to UV light for 30–60 s.

! **CAUTION** Avoid direct exposure to UV light; it is mutagenic.

▲ **CRITICAL STEP** Keep the exposed pins clean, as dirt can break or ruin the connection to electronic equipment.

Device surface treatment ● **TIMING 5–10 min**

40| Prepare the surface-treatment solution required for all droplet operations. We typically use option A, but if droplet generation is hampered as a result of wetting effects, option B should be applied.

(A) Preparation of Aquapel water-repellent solution

- (i) The Aquapel solution is supplied in a glass ampule embedded in a thick felt pad. Carefully cut the pad and remove the ampule.
- (ii) Place the ampule at the bottom of a 15-ml Falcon-type conical plastic tube and score the ampule using a diamond pen or similar. Carefully break the ampule inside the tube.
- (iii) Transfer the Aquapel solution into a 5-ml glass, gas-tight syringe, while leaving the broken glass in the 15-ml plastic tube.

▲ **CRITICAL STEP** Remove air bubbles from the syringe. Upon prolonged contact with air, Aquapel precipitates and loses its functionality. Aquapel can be stored for up to ~2 weeks by preventing air contact.

(B) Preparation of perfluorododecyltrichlorosilane water-repellent solution

- (i) Transfer 1% (vol/vol) perfluorododecyltrichlorosilane solution (Reagent Setup) into a glass syringe.

41| Attach a 0.22- μ m Millipore filter and a 23-gauge needle to the syringe and affix PTFE microtubing to the needle.



PROTOCOL

42| Insert the microtube into the continuous-phase inlet of a single microfluidic module, and then inject the surface-treatment solution to fill each of the device channels.

43| Leave the solution in the channels for 10–30 s, and then flush with pressurized air or nitrogen.

44| Rinse the microfluidic channels with pure FC-40 oil to remove the unreacted silane, and then flush every module with pressurized air or nitrogen.

? TROUBLESHOOTING

■ **PAUSE POINT** Devices can be stored at room temperature for weeks or months before use. To prevent degradation of treated surfaces, avoid direct sunlight. Device surfaces should be covered with Scotch tape to keep dust from the openings.

Preparation of 9E10 cells ● TIMING 30 min

45| Maintain 9E10 cell lines in complete DMEM prewarmed at 37 °C in 5% CO₂, at ~3 × 10⁵ cells per ml. Subculture the cell lines every 3 d.

46| 9E10 cells grow as semiadherent cells and can be passaged by transferring a fraction of the cells growing in suspension (typically 2 ml) to a fresh flask containing 18 ml of prewarmed culture medium.

47| Remove an aliquot of 9E10 cell culture supernatant and count the cells using a hemocytometer.

48| Transfer a volume of the cell culture supernatant that contains an excess of the cells required (>2 × 10⁵, as some cells will be lost during centrifugation) to a 15-ml conical tube.

49| Centrifuge the cells at 350g for 5 min and carefully remove all growth medium from the cell pellet. Resuspend the cells in 10 ml of cold complete DMEM and use a hemocytometer to count the cells.

50| Transfer 1.4 × 10⁵ cells to a fresh tube on ice.

51| Centrifuge the cells at 350g for 5 min and carefully remove all growth medium from the cell pellet.

52| Add 84 μl of ice-cold complete DMEM and 16 μl of OptiPrep density-gradient medium to the cells. Pipette gently to mix, and then keep the cells on ice until the suspension is combined with the K562 cell preparation described in Steps 54–62 below.

▲ **CRITICAL STEP** Avoid cell damage during handling, as damaged cells release chromosomal DNA that entraps multiple cells and forms clusters that can clog the microfluidic filters.

53| (Optional) If DNA is released from disrupted cells and it interferes with microfluidic operations, the cell suspension can be treated with DNase I (provided that subsequent operations do not involve DNA amplification or analysis). In this case, pellet the cells by centrifugation at 350g for 5 min at room temperature, resuspend in 2 ml of DNase solution and leave the suspension at room temperature for 15 min. After the treatment, centrifuge the cells at 350g for 5 min at room temperature and carefully remove all supernatant from the cell pellet. Wash cells twice in 10 ml of cold complete DMEM and resuspend the cells in ~5 ml of ice-cold complete DMEM; place the cells on ice for 10 min.

Preparation and staining of K562 cells ● TIMING 1 h

54| Maintain K562 cell lines in complete DMEM prewarmed at 37 °C in 5% CO₂, at ~3 × 10⁵ cells per ml. Subculture the cell lines every 3 d.

55| K562 cells grow in suspension and should be diluted ~1/10 every 3 d to maintain a cell concentration of ~3 × 10⁵ cells per ml.

56| Remove an aliquot of K562 cell culture supernatant and count the cells using a hemocytometer. Transfer a volume of cell culture supernatant that contains an excess of the cells required (>2 × 10⁶, as some cells will be lost during centrifugation) to 15-ml conical tube(s).

57| Pellet the cells by centrifugation at 350g for 5 min and replace all supernatant with 10 ml of DMEM prewarmed at 37 °C, not supplemented with FBS or antibiotic, containing 0.2 μM CMRA dye.

58| Incubate the cell suspension at 37 °C in 5% CO₂ for 30 min.

59| Pellet the cells by centrifugation at 350*g* for 5 min and replace all supernatant with 10 ml of complete DMEM (prewarmed at 37 °C). Transfer ~1.4 × 10⁶ cells to a 15-ml conical tube and incubate the cells at 37 °C in 5% CO₂ for 10 min.

60| Place the cells on ice for 10 min.

61| Pellet the cells and carefully remove all supernatant. Resuspend the pellet in 84 μl of ice-cold complete DMEM and add 16 μl of OptiPrep medium.

62| Combine the 100-μl 9E10 cell preparation from Steps 45–53 with the 100-μl K562 cell preparation to generate a suspension with a 1:10 ratio of 9E10:K562 cells.

Preparation of beads ● TIMING 1.5 h

63| Transfer ~4 × 10⁶ streptavidin-coated beads to a fresh 1.5-ml Eppendorf tube (use the manufacturer's data sheet to determine concentration of supplied beads or count them using a hemocytometer).

64| Centrifuge the beads for 1 min at 2,000*g* at room temperature, carefully remove the supernatant with a 200-μl pipette, and then resuspend the beads in 100 μl of PBS. Repeat this step twice to complete initial washing.

65| Pellet the beads by centrifugation using the same settings as in Step 64 and remove all supernatant. Resuspend the beads in 200 μl of PBS with 13 μg of biotinylated capture antibody and incubate for ~60 min with shaking at room temperature.

66| Wash the beads once with 200 μl of 0.05% (vol/vol) Triton X-100 in PBS and three times with 200 μl of complete DMEM.

67| Resuspend the beads in 161.5 μl of complete DMEM and mix with 32 μl of OptiPrep medium and 6.5 μl of detection antibody (1 μg μl⁻¹, corresponding to ~2.4 × 10¹³ antibody molecules).

Cell encapsulation ● TIMING 1 h

68| Place 300 μl of pure HFE-7500 oil in a sterile 1-ml syringe. Transfer the 200-μl 9E10/K562 cell suspension to the oil surface using a pipette. The density of the cell suspension (~1.1 g m⁻³) is lower than that of HFE-7500 (1.614 g m⁻³), and it will remain on top of the oil.

69| Place a 23-gauge needle on the syringe, connect it to PTFE microtubing and place it on a vertically oriented syringe pump with the needle facing upward.

▲ **CRITICAL STEP** Use an ice-cold jacket to cool the syringe containing the cells during the encapsulation step. This strategy minimizes cell secretion during the encapsulation process.

70| In the same way as in Steps 68 and 69, load a second syringe with the mixture containing antibody-capture beads and the labeling antibody.

71| Prepare a third syringe for the continuous phase, with HFE-7500 oil containing 1.5% (wt/wt) fluorinated surfactant.

72| Connect the syringes to the corresponding inlets of the microfluidic chip via PTFE microtubing and start infusing. Use flow rates of 90 μl h⁻¹ for the cell suspension, 90 μl h⁻¹ for the bead solution and 180 μl h⁻¹ for the continuous phase. When using this chip design (provided as **Supplementary Data**) and 25-μm-deep channels, 50-pl droplets should be generated at ~1,000 droplets per second (**Supplementary Video 1** and **Supplementary Fig. 1**).

? TROUBLESHOOTING

73| In order to collect the encapsulated cells, connect PTFE microtubing to the device exit and place the tubing outlet inside a vertically oriented 1-ml syringe or in a 1.5-ml Eppendorf-type tube. In either case, prefill the collection vessel with 100 μl of the continuous phase and place the tubing outlet in this fluid. This maneuver prevents droplet breakage due to contact with dry surfaces. A cooling jacket should be used to keep the collection vessel at ~4 °C.

? TROUBLESHOOTING

PROTOCOL

Emulsion storage off-chip ● TIMING 15–30 min

74| After the encapsulated cell/bead emulsion is collected, place the collection vessel in a cell culture incubator for 15 min to facilitate antibody secretion.

▲ **CRITICAL STEP** The air in the incubator should be water saturated to prevent evaporation from the top layer of droplets.

Analysis of droplets ● TIMING 5–10 min

75| Droplets are easily visualized by the use of Vitrocom glass capillary tubes. Prewet a tube by quickly dipping the end into HFE-7500 containing surfactant. Touch the same end into the surface of the droplet emulsion. Droplets will quickly wick into the capillary.

76| Lay the tube on a microscope slide and seal the tube ends with vacuum grease. Droplets can now be easily observed by microscopy. Alternatively, a hemocytometer or standard glass slide and microscope cover slip can be used to trap and observe drops; however, care must be taken to prevent droplet evaporation and merging.

77| Count the number of occupied droplets. If droplets have been incubated at 37 °C for >15 min, fluorescence microscopy can be used to observe and count the droplets that contain a bead made fluorescent by the presence of an antibody-secreting cell.

? TROUBLESHOOTING

Droplet sorting ● TIMING 1–6 h

78| Place the droplet-sorting device on a microscope stage and connect the positive and negative electrodes to the high-voltage amplifier. The positive and negative electrodes are marked in **Figure 2** with '+' and '-' signs, respectively.

! **CAUTION** The negative electrode should be grounded for safety.

79| Attach the ITO surface of a microfluidic chip (facing the microscope stage) to the ground electrode using alligator or similar clips.

80| Attach a 27.5-gauge needle to the emulsion-containing syringe, insert PTFE microtubing and place it on a syringe pump with the needle facing up. Set the infusion rate to 500 $\mu\text{l h}^{-1}$ and push the emulsion through the tubing until it reaches the end. Stop the flow and insert the tubing into the injection port of the microfluidic device.

81| Connect a second 2.5-ml syringe filled with HFE-7500 oil containing 1.5% (wt/wt) fluorinated surfactant to the oil inlet of the device and infuse at 200 $\mu\text{l h}^{-1}$. Set the emulsion flow rate at 50 $\mu\text{l h}^{-1}$, until the droplets enter the device channels and then reduce the flow rate to 20 $\mu\text{l h}^{-1}$. Allow a few minutes for the flow inside the microfluidic chip to stabilize.

? TROUBLESHOOTING

82| Set the oil and emulsion flow rates at 480 $\mu\text{l h}^{-1}$ and 20 $\mu\text{l h}^{-1}$, respectively. At these rates, droplets are sufficiently spaced by the carrier oil and will not collide at the sorting junction (**Supplementary Video 2**).

83| Move the microscope field of view to the sorting junction (**Fig. 2b**). All droplets should flow into the negative arm (waste channel). Increase the continuous-phase flow rate if some droplets flow into the sort channel while the electrodes are off.

84| Focus the laser spot of the optical setup (**Fig. 6**) on the section of channel above the triangular fiducial mark (**Fig. 2b**, red triangle in inset 5). Start LabVIEW and load the custom data acquisition and control software. Fluorescence traces corresponding to droplets should become visible on the data acquisition software. Adjust the focus and laser spot position to obtain the highest signal-to-noise ratio for fluorescence peaks.

! **CAUTION** Wear proper safety goggles when operating the laser and ensure that the laser has appropriate safety interlocks.

85| By using LabVIEW software, adjust the detection threshold so that all green fluorescent droplets are detected.

? TROUBLESHOOTING

86| Tune the sorting parameters. We apply a burst of 60 square pulses with an amplitude of 0.6–0.8 kV, output frequency of 30 kHz and sorting delay of 100 μs .

87| Reduce the sorting threshold to the same level as the detection threshold. Upon electrode activation, all the droplets should be directed into the positive arm (collection channel), thus confirming effective dielectrophoretic sorting. Repeat

Steps 84 and 86, adjusting the sorting parameters as necessary, until droplets are sorted reproducibly into the collection channel only when the sorting signal is applied.

? TROUBLESHOOTING

88| Once proper sorting conditions are identified (**Supplementary Video 3**), install collection tubing and collection tubes, set the desired sorting threshold and sort the droplets until the desired number of droplets are collected.

89| (Optional) Use a high-speed camera (e.g., Phantom V7.2) to record digital movies during the sorting and observe the sorting errors. We strongly recommend implementing this optional step because it enables monitoring of the sorting process so that relevant parameters can be adjusted as needed.

90| After sorting is complete, turn off the electrodes, unplug the collection tubing from the microfluidic device and let the oil from the tubing drain into a collection tube. In this way, droplets that were trapped inside the tubing will be collected without any loss.

Analysis of sorted droplets ● **TIMING ~1 h**

91| Aqueous droplets float on HFE 7500 oil; therefore, sorted droplets accumulate at the air-oil interface in the collection tube. A layer of droplets should be visible after sorting. Use the Vitrocom glass capillary tubes as described in Step 75 to prepare the droplets for imaging using fluorescence microscopy.

92| Calculate the enrichment of antibody-secreting cells using the following equation^{52,93}:

$$\eta = \frac{N_{+1}/N_{-1}}{N_{+0}/N_{-0}}$$

where η is enrichment, N_{+0} and N_{+1} are the number of antibody-secreting (9E10) cells present before and after sorting, respectively; N_{-0} and N_{-1} are the number of negative cells that do not secrete antibodies (in this case, K562) before and after sorting, respectively.

Breaking the emulsion (optional) ● **TIMING 10–30 min**

▲ **CRITICAL** Steps 93–97 should be implemented if the experimenter is planning to perform a separate analysis on sorted cells.

93| Cells trapped inside the droplets should be released before propagation in a cell culture dish or before analysis using conventional techniques²⁶. For this purpose, first add 500 μ l of fresh cell culture medium on top of the sorted droplets.

94| Add a volume of PFO equal to the volume of the continuous phase.

95| Gently mix the PFO with the continuous phase by tapping the tube with a finger.

96| Leave the tube on the bench for 1–2 min. Once droplets are broken, the interface between oil and growth medium becomes clear and the two phases appear completely separate.

? TROUBLESHOOTING

97| Spin the tube at 60g for 10 s at room temperature to fully separate the two phases. Collect the supernatant containing the cells and transfer it to a cell culture flask or microtiter plate well. Do not spin the tube longer or with higher force, as this may pin the cells to the oil phase and reduce the yield.

? TROUBLESHOOTING

? TROUBLESHOOTING

Troubleshooting advice can be found in **Table 1**.

TABLE 1 | Troubleshooting table.

Step	Problem	Possible reason	Solution
9	The resist has wrinkles on its surface	The solvent is not completely evaporated during the initial baking step	Repeat Steps 7 and 9 until wrinkles are no longer visible upon cooling to room temperature
12	Cracks in the SU-8 film	Rapid substrate cooling may create thermal stresses in the SU-8 film that result in cracking	Cool the wafer more slowly by placing it on a thermally insulating surface to cool, or by turning the hot plate off and allowing the wafer and hot plate to cool down together Hard baking may also reduce the appearance of cracks (see Step 16)
13	SU-8 structures are of poor quality or undeveloped resist remains trapped between the SU-8 features	Insufficient contact between the mask and substrate during UV exposure (Step 10)	Assure the direct contact between the mask and substrate (follow the instructions of your UV light source exposure system)
23	SU-8 structures detach from the wafer during PDMS peeling	Developing step is too short (Step 13)	Increase the developing time
		Insufficient UV light source exposure time	Check exposure time in Step 10 (see Microchem SU-8 data sheet available online http://www.microchem.com/Prod-SU8_KMPR.htm)
		Wafer was not clean	Follow the procedure detailed in Step 4 to clean the surface of the wafer
	PDMS does not peel properly from SU-8 structures	Insufficient baking	Increase the baking time (Steps 11 and 12)
25	Device leaks	Punch was not sharp enough	Use a new punch
	Molten solder backflows around the solder wire	Chosen punch size is too large	Smaller holes will prevent molten solder from backflowing around the solder wire, as it is inserted into the microchannel
31	Device delaminates	Glass slide is not clean	Rinse the glass slide with acetone, isopropanol and methanol, and then blow-dry with pressurized nitrogen
		Plasma treatment was suboptimal	Make sure that parameters of your plasma machine are set correctly and that oxygen gas is flowing properly into the chamber
32	Channels have collapsed	Microfluidic channels can collapse if too much force is applied	Apply less force when sealing PDMS slab to the glass
37	Microelectrodes show no conductivity	Air bubbles are trapped inside microelectrode channel	Place device on a hot plate set at 90 °C and bake for 10 min. If this does not help, there is no connection between electrodes and wires
		No connection between microelectrodes and wires	Remove the pin and repeat microelectrode manufacturing (Steps 34–37)
44	Aqueous components wet the walls of the microfluidic channel	Inefficient surface treatment	Repeat surface treatment (Steps 40–44)

(continued)

TABLE 1 | Troubleshooting table (continued).

Step	Problem	Possible reason	Solution
72	Cells clump inside microfluidic device	The DNA released from dead cells causes cell clumping	Be very gentle when preparing the cells before encapsulation (see Steps 45–52 for 9E10 cells and Steps 54–62 for K562 cells) Use DNase I or restriction endonucleases for digestion, if possible (Step 53)
	Cells stop entering microfluidic device after few minutes of operation	Cells are clumping	Use the right amount of density-matching solution (OptiPrep or similar) to adjust the density of the aqueous phase
73	Droplets coalesce at the outlet	Surfactant concentration is too low	Increase the surfactant concentration until no coalescence is observed
		Inefficient surfactant	Purchase or synthesize new surfactant
77	Beads show high fluorescence background signal	Cell suspension contains many dead cells, which release internal antibodies	Prepare a fresh sample of cells with more care (Steps 45–52)
81	Droplets coalesce during re-injection	Poor stabilization by surfactant	Make sure that droplets entering collection outlet are stable Check whether there is any dust or pieces of PDMS in the re-injection inlet Make sure that tubing inserted into the device does not squeeze droplets. Tubing should be inserted to one-third or one-half the thickness of the PDMS Be careful when inserting tubing on the needle. Inner walls of tubing can be easily scratched by the tip of the needle and create a plug that will block the flow of droplets When re-injecting emulsion, avoid using flow rates higher than 500 $\mu\text{l h}^{-1}$
87	Sorting does not work	Microelectrode malfunction	Follow steps to prepare microelectrodes (Steps 34–38)
		Wrong sorting parameters	Increase the voltage and pulse duration applied on electrodes to direct droplets into sorting channel
		The wrong droplets are sorted	Check sorting delay (the time from detection of droplet fluorescence to applied sorting pulse)
	Droplets break during sorting	Droplets break due to increased shear force	Reduce the sorting voltage applied on the electrodes
96	Emulsion does not break	Poor mixing of perfluorooctanol with carrier oil	Make sure that perfluorooctanol is properly mixed with carrier oil Use two volumes or more of perfluorooctanol for one volume of carrier oil
97	Released cells are dead	The procedure causes cytotoxic effects	Although cells can stay alive on perfluorinated liquids, vigorous mixing of encapsulated cells with perfluorooctanol can lead to cell death Ensure proper gas exchange
		Cells have consumed most of the nutrients inside droplets	To extend the life span of cells inside droplets, encapsulated cells should be kept on ice during all off-chip operations

● TIMING

Steps 1 and 2, mask design and ordering: 1–5 d

Steps 3–17, master fabrication: ~1 h



PROTOCOL

Steps 18–33, preparation of the PDMS mold: 2–12 h
Steps 34–39, microelectrode manufacture: 10–30 min
Steps 40–44, device surface treatment: 5–10 min
Steps 45–53, preparation of 9E10 cells: 30 min
Steps 54–62, preparation and staining of K562 cells: 1 h
Steps 63–67, preparation of beads: 1.5 h
Steps 68–73, cell encapsulation: 1 h
Step 74, emulsion storage off-chip: 15–30 min
Steps 75–77, analysis of droplets: 5–10 min
Steps 78–90, droplet sorting: 1–6 h
Steps 91 and 92, analysis of sorted droplets: 1 h
Steps 93–97, breaking the emulsion (optional): 10–30 min
Box 2, droplet screening instrument optical alignment procedure: 1–2 d

ANTICIPATED RESULTS

Upon completion of the experiments described in this protocol, one should be able to manufacture droplet-based microfluidic chips and use them for single-cell analysis and sorting in a high-throughput manner.

As a specific example, here we describe a binding assay to detect antibody production from single mouse hybridoma cells. We use two cell types, 9E10 cells and K562 cells, at densities in which the latter are present at an approximately tenfold excess. Single cells are co-compartmentalized in 50- μ l droplets together with 6- μ m-diameter beads coated with antibodies directed against the Fc fragment of mouse IgG antibodies. A labeling probe (antibody directed against the Fab fragment of mouse IgG antibodies and labeled with DyLight 488 fluorescent dye), is also co-compartmentalized in the droplets. Mouse IgG antibodies secreted from single cells in droplets are detected using a sandwich assay, which, in contrast to standard ELISA assays, does not require any washing steps.

Secreted antibodies are captured on the bead surface, and they recruit the labeling probe that is present in the same droplet (**Fig. 4**). In the absence of binding activity, the fluorescence signal remains distributed over the entire droplet volume, but, upon binding, the fluorescent probe becomes concentrated onto a bead, leading to a clearly distinguishable fluorescence spike (**Fig. 5**). Because of the small reaction volumes, the secreted antibodies can reach detectable levels within 15 min. The rate of antibody secretion per cell over the first 30 min was measured to be $\sim 4 \times 10^4$ molecules per cell per minute, resulting in high and detectable concentrations (~ 20 nM) after only 15 min.

Confinement in droplets can, however, also impose some strain on the cells. Depletion of the nutrients inside the droplet may impair cell functions or even cause cell death. To slow cellular metabolism, we keep encapsulated cells at 4 °C during all the microfluidic steps and induce protein secretion by shifting the emulsion to 37 °C for ~ 15 –30 min. Droplets containing fluorescent beads were dielectrophoretically sorted at ~ 200 Hz frequency, using a microfluidic chip (**Fig. 2b**) whose design is provided as **Supplementary Data**.

We used a custom LabVIEW script that detects fluorescence intensity and sends short electric pulses to the electrodes to direct droplets into the collection channel as they pass the sorting junction (**Supplementary Video 3**). The sorting threshold was set such that all the droplets having a fluorescence intensity three times higher than the background signal were sorted and collected off-chip into an Eppendorf tube. Approximately 1,000 sorted droplets were then imaged using a fluorescence microscope. We calculate the enrichment, η , as

$$\eta = \frac{N_{+,1}}{N_{-,1}} \bigg/ \frac{N_{+,0}}{N_{-,0}} = \frac{\epsilon_1}{\epsilon_0}$$

where $N_{+,1}$ is the number of ‘positive’ 9E10 cells and $N_{-,1}$ is the number of ‘negative’ K562 cells after the sorting process. Correspondingly, $N_{+,0}$ is the number of positive 9E10 cells and $N_{-,0}$ is the number of negative K562 cells before sorting. After a single round of sorting, we obtained ~ 220 -fold enrichment of 9E10 hybridoma cells (**Fig. 7** and **Table 2**). According to statistical modeling of cell encapsulation⁹⁴ and sorting⁵², the enrichment in heterogeneous cell mixtures (composed of two or more cell types) is limited by the coencapsulation probability of positive and negative cells. During the sorting step, droplets having at least one positive cell will be sorted regardless of the number of negative cells coencapsulated into the same droplet. After sorting, out of over 1,000 droplets analyzed, only one contained a single negative cell, whereas 47 droplets contained at least one positive and one negative cell (**Table 2**). At the expense of reducing throughput, enrichment can be further improved by diluting the initial cell mixture to $\lambda = 0.1$ (or less), as at low λ values coencapsulation events become negligible.

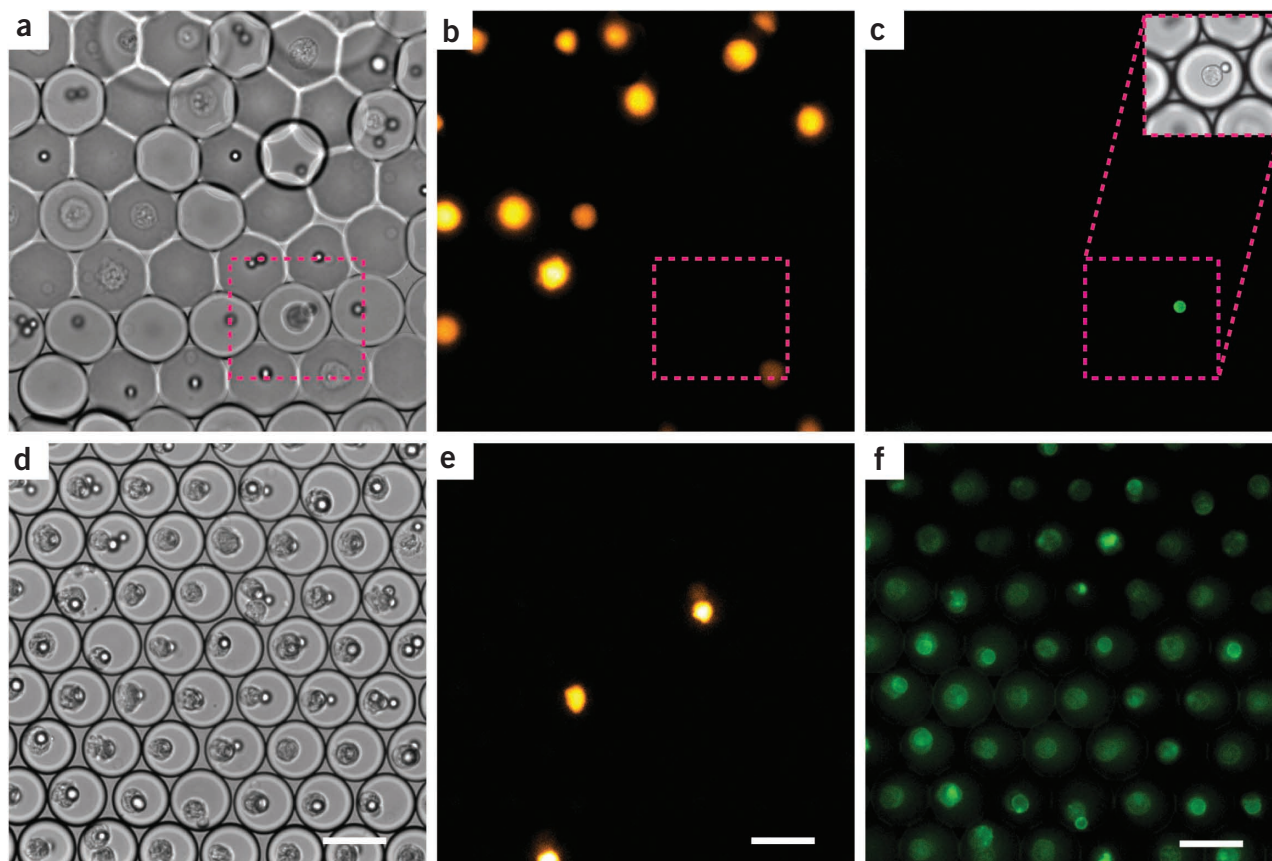


Figure 7 | Compartmentalized single hybridoma cells before and after microfluidic sorting. (a–f) The upper row shows micrographs of droplets after incubation at 37 °C for 15 min and the lower row shows droplets after microfluidic sorting. (a,d) Bright-field images. (b,e) Orange fluorescence, which is due to the presence of K562 cells. (c,f) Green fluorescence, due to 9E10-secreted antibodies binding to the beads. The green fluorescence signal on the beads is the result of 9E10-secreted antibodies captured on the beads by an anti-mouse Fc antibody and then in turn bound by a green fluorescence-labeled goat anti-mouse-F(ab)2 antibody. These binding events result in the green fluorescent anti-mouse-F(ab)2 antibody becoming concentrated on the beads instead of being distributed homogeneously throughout the volume of the droplet. The assay is therefore similar in nature to a sandwich ELISA, but it relies on the detection of the bead-bound detection antibody, rather than the measurement of detection antibodies after washing, as in ELISA. Note that in d, some beads are not clearly visible, as they occupy a different focal plane. The pink dashed box shows a droplet containing a 9E10 cell and a green fluorescent bead. Scale bars, 50 μm.

The microfluidic system described is easily adapted to the screening of other cell types, including bacteria^{32,52}, yeast⁴⁵, insect³³ or other mammalian cells^{25–27,70,80,95}. The system can also be tailored to screen for other activities. For example, antibodies (or other proteins) can also be screened for inhibitory activities²². In this case, the beads are omitted and the enzyme to be inhibited is coencapsulated directly with the cells. After incubation, a fluorogenic substrate can be added by drop fusion, and then fluorescence can be measured after a short incubation. Adapting the system to the detection of the catalytic activity of intracellular, cell-surface or secreted proteins is even easier. For cell-surface or secreted proteins, the cells are co-compartmentalized directly with a fluorogenic substrate⁴⁵. The procedure is easily modified for screening intracellular proteins: if required, cell lysis agents are added to the cells immediately before compartmentalization in droplets^{19,46}.

TABLE 2 | Sorting results.

	Droplets with a single 9E10 cell	Droplets with two or more 9E10 cells	Droplets with a single K562 cell	Droplets with two or more K562 cells	Droplets containing at least one 9E10 and one K562 cell	Droplets with no cells
Before sorting	320	0	2,480	300	8	~10,000 (~60% empty)
After sorting	948	31 ^a	1	0	47	6

^aDroplets having two or more 9E10 cells may have been preferentially enriched because a higher number of cells will secrete more antibody and therefore will lead to higher bead fluorescence.



Note: Supplementary information is available in the [online version of the paper](#).

ACKNOWLEDGMENTS We are grateful to R. Sperling for the kind gift of surfactant and D. Aubrecht for his help in developing droplet detection and sorting methods. This work was supported by the National Science Foundation (NSF) (DMR-1006546), the National Institutes of Health (NIH) (P01GM096971 and 5R01EB014703-02), the Harvard Materials Science Research and Engineering Center (DMR-0820484) and the Lithuanian Research Council (MIP-048/2012). W.L.U. acknowledges support from a Canadian National Sciences and Engineering Research Council (NSERC) Postgraduate Scholarship (PGS D). J.A.H. and J.G. were supported by NIH SBIR grant no. 1R43AI082861-01. This work was performed in part at the Center for Nanoscale Systems (CNS), a member of the National Nanotechnology Infrastructure Network (NNIN), which is supported by the NSF under award no. ECS-0335765. CNS is part of Harvard University.

AUTHOR CONTRIBUTIONS L.M. and J.A.H. performed the experiments described in this protocol, W.L.U. provided the LabVIEW software, L.M., J.A.H. and A.D.G. analyzed the data; J.G. set up the detection system, all authors edited and proofread the paper.

COMPETING FINANCIAL INTERESTS

The authors declare competing financial interests: details are available in the [online version of the paper](#).

Reprints and permissions information is available online at <http://www.nature.com/reprints/index.html>.

1. Guo, M.T., Rotem, A., Heyman, J.A. & Weitz, D.A. Droplet microfluidics for high-throughput biological assays. *Lab Chip* **12**, 2146–2155 (2012).
2. Kintses, B., van Vliet, L.D., Devenish, S.R. & Hollfelder, F. Microfluidic droplets: new integrated workflows for biological experiments. *Curr. Opin. Chem. Biol.* **14**, 548–555 (2010).
3. Theberge, A.B. *et al.* Microdroplets in microfluidics: an evolving platform for discoveries in chemistry and biology. *Angew. Chem. Int. Ed.* **49**, 5846–5868 (2010).
4. Dove, A. Drug screening—beyond the bottleneck. *Nat. Biotechnol.* **17**, 859–863 (1999).
5. Link, D.R., Anna, S.L., Weitz, D.A. & Stone, H.A. Geometrically mediated breakup of drops in microfluidic devices. *Phys. Rev. Lett.* **92**, 054503 (2004).
6. Mazutis, L., Baret, J.C. & Griffiths, A.D. A fast and efficient microfluidic system for highly selective one-to-one droplet fusion. *Lab Chip* **9**, 2665–2672 (2009).
7. Mazutis, L. & Griffiths, A.D. Selective droplet coalescence using microfluidic systems. *Lab Chip* **12**, 1800–1806 (2012).
8. Ahn, K., Agresti, J., Chong, H., Marquez, M. & Weitz, D.A. Electrocoalescence of drops synchronized by size-dependent flow in microfluidic channels. *Appl. Phys. Lett.* **88**, 264105–264103 (2006).
9. Chabert, M., Dorfman, K.D. & Viovy, J.L. Droplet fusion by alternating current (AC) field electrocoalescence in microchannels. *Electrophoresis* **26**, 3706–3715 (2005).
10. Priest, C., Herminghaus, S. & Seemann, R. Controlled electrocoalescence in microfluidics: targeting a single lamella. *Appl. Phys. Lett.* **89**, 134101 (2006).
11. Abate, A.R., Hung, T., Mary, P., Agresti, J.J. & Weitz, D.A. High-throughput injection with microfluidics using picoinjectors. *Proc. Natl. Acad. Sci. USA* **107**, 19163–19166 (2010).
12. Li, L. *et al.* Nanoliter microfluidic hybrid method for simultaneous screening and optimization validated with crystallization of membrane proteins. *Proc. Natl. Acad. Sci. USA* **103**, 19243–19248 (2006).
13. Niu, X., Gulati, S., Edel, J.B. & deMello, A.J. Pillar-induced droplet merging in microfluidic circuits. *Lab Chip* **8**, 1837–1841 (2008).
14. Frenz, L., Blank, K., Brouzes, E. & Griffiths, A.D. Reliable microfluidic on-chip incubation of droplets in delay-lines. *Lab Chip* **9**, 1344–1348 (2009).
15. Hatch, A.C. *et al.* 1-Million droplet array with wide-field fluorescence imaging for digital PCR. *Lab Chip* **11**, 3838–3845 (2011).
16. Shim, J.U. *et al.* Simultaneous determination of gene expression and enzymatic activity in individual bacterial cells in microdroplet compartments. *J. Am. Chem. Soc.* **121**, 15251–15256 (2009).
17. Mazutis, L. *et al.* Droplet-based microfluidic systems for high-throughput single DNA molecule isothermal amplification and analysis. *Anal. Chem.* **81**, 4813–4821 (2009).
18. Lichtman, J.W. & Conchello, J.A. Fluorescence microscopy. *Nat. Methods* **2**, 910–919 (2005).

19. Najah, M., Griffiths, A.D. & Ryckelynck, M. Teaching single-cell digital analysis using droplet-based microfluidics. *Anal. Chem.* **84**, 1202–1209 (2012).
20. Ahn, K. *et al.* Dielectrophoretic manipulation of drops for high-speed microfluidic sorting devices. *Appl. Phys. Lett.* **88**, 024104 (2006).
21. Franke, T., Abate, A.R., Weitz, D.A. & Wixforth, A. Surface acoustic wave (SAW) directed droplet flow in microfluidics for PDMS devices. *Lab Chip* **9**, 2625–2627 (2009).
22. Debs, B.E., Utharala, R., Balyasnikova, I.V., Griffiths, A.D. & Merten, C.A. Functional single-cell hybridoma screening using droplet-based microfluidics. *Proc. Natl. Acad. Sci. USA* **109**, 11570–11575 (2012).
23. Granieri, L., Baret, J.C., Griffiths, A.D. & Merten, C.A. High-throughput screening of enzymes by retroviral display using droplet-based microfluidics. *Chem. Biol.* **17**, 229–235 (2010).
24. He, M. *et al.* Selective encapsulation of single cells and subcellular organelles into picoliter- and femtoliter-volume droplets. *Anal. Chem.* **77**, 1539–1544 (2005).
25. Clausell-Tormos, J. *et al.* Droplet-based microfluidic platforms for the encapsulation and screening of mammalian cells and multicellular organisms. *Chem. Biol.* **15**, 427–437 (2008).
26. Koster, S. *et al.* Drop-based microfluidic devices for encapsulation of single cells. *Lab Chip* **8**, 1110–1115 (2008).
27. Brouzes, E. *et al.* Droplet microfluidic technology for single-cell high-throughput screening. *Proc. Natl. Acad. Sci. USA* **106**, 14195–14200 (2009).
28. Liu, W., Kim, H.J., Lucchetta, E.M., Du, W. & Ismagilov, R.F. Isolation, incubation, and parallel functional testing and identification by FISH of rare microbial single-copy cells from multi-species mixtures using the combination of chemistode and stochastic confinement. *Lab Chip* **9**, 2153–2162 (2009).
29. Hufnagel, H. *et al.* An integrated cell culture lab on a chip: modular microdevices for cultivation of mammalian cells and delivery into microfluidic microdroplets. *Lab Chip* **9**, 1576–1582 (2009).
30. Zeng, Y., Novak, R., Shuga, J., Smith, M.T. & Mathies, R.A. High-performance single cell genetic analysis using microfluidic emulsion generator arrays. *Anal. Chem.* **82**, 3183–3190 (2010).
31. Rane, T.D., Zec, H.C., Puleo, C., Lee, A.P. & Wang, T.H. Droplet microfluidics for amplification-free genetic detection of single cells. *Lab Chip* **12**, 3341–3347 (2012).
32. Huebner, A. *et al.* Development of quantitative cell-based enzyme assays in microdroplets. *Anal. Chem.* **80**, 3890–3896 (2008).
33. Baret, J.C., Beck, Y., Billas-Massobrio, I., Moras, D. & Griffiths, A.D. Quantitative cell-based reporter gene assays using droplet-based microfluidics. *Chem. Biol.* **17**, 528–536 (2010).
34. Huebner, A. *et al.* Quantitative detection of protein expression in single cells using droplet microfluidics. *Chem. Commun. (Camb)* **28**, 1218–1220 (2007).
35. Chen, D. *et al.* The chemistode: a droplet-based microfluidic device for stimulation and recording with high temporal, spatial, and chemical resolution. *Proc. Natl. Acad. Sci. USA* **105**, 16843–16848 (2008).
36. Niu, X., Gielen, F., Edel, J.B. & deMello, A.J. A microdroplet dilutor for high-throughput screening. *Nat. Chem.* **3**, 437–442 (2011).
37. Mazutis, L. *et al.* Multi-step microfluidic droplet processing: kinetic analysis of an *in vitro*-translated enzyme. *Lab Chip* **9**, 2902–2908 (2009).
38. Pekin, D. *et al.* Quantitative and sensitive detection of rare mutations using droplet-based microfluidics. *Lab Chip* **11**, 2156–2166 (2011).
39. Zhong, Q. *et al.* Multiplex digital PCR: breaking the one target per color barrier of quantitative PCR. *Lab Chip* **11**, 2167–2174 (2011).
40. Hindson, B.J. *et al.* High-throughput droplet digital PCR system for absolute quantitation of DNA copy number. *Anal. Chem.* **83**, 8604–8610 (2011).
41. Tewhey, R. *et al.* Microdroplet-based PCR enrichment for large-scale targeted sequencing. *Nat. Biotechnol.* **27**, 1025–1031 (2009).
42. Miller, O.J. *et al.* High-resolution dose-response screening using droplet-based microfluidics. *Proc. Natl. Acad. Sci. USA* **109**, 378–383 (2012).
43. Clausell-Tormos, J., Griffiths, A.D. & Merten, C.A. An automated two-phase microfluidic system for kinetic analyses and the screening of compound libraries. *Lab Chip* **10**, 1302–1307 (2010).
44. Churski, K. *et al.* Rapid screening of antibiotic toxicity in an automated microdroplet system. *Lab Chip* **12**, 1629–1637 (2012).
45. Agresti, J.J. *et al.* Ultrahigh-throughput screening in drop-based microfluidics for directed evolution. *Proc. Natl. Acad. Sci. USA* **107**, 4004–4009 (2010).
46. Kintses, B. *et al.* Picoliter cell lysate assays in microfluidic droplet compartments for directed enzyme evolution. *Chem. Biol.* **19**, 1001–1009 (2012).



47. Paegel, B.M. & Joyce, G.F. Microfluidic compartmentalized directed evolution. *Chem. Biol.* **17**, 717–724 (2010).
48. Lowe, K.C. Perfluorochemical respiratory gas carriers: benefits to cell culture systems. *J. Fluorine Chem.* **118**, 19–26 (2002).
49. Scott, R.L. The solubility of fluorocarbons. *J. Am. Chem. Soc.* **70**, 4090–4093 (1948).
50. Simons, J.H. & Linevsky, M.J. The solubility of organic solids in fluorocarbon derivatives. *J. Am. Chem. Soc.* **74**, 4750–4751 (1952).
51. Tawfik, D.S. & Griffiths, A.D. Man-made cell-like compartments for molecular evolution. *Nat. Biotechnol.* **16**, 652–656 (1998).
52. Baret, J.C. *et al.* Fluorescence-activated droplet sorting (FADS): efficient microfluidic cell sorting based on enzymatic activity. *Lab Chip* **9**, 1850–1858 (2009).
53. Martino, C. *et al.* Intracellular protein determination using droplet-based immunoassays. *Anal. Chem.* **83**, 5361–5368 (2011).
54. Beer, N.R. *et al.* On-chip single-copy real-time reverse-transcription PCR in isolated picoliter droplets. *Anal. Chem.* **80**, 1854–1858 (2008).
55. Schaeferli, Y. *et al.* Continuous-flow polymerase chain reaction of single-copy DNA in microfluidic microdroplets. *Anal. Chem.* **81**, 302–306 (2009).
56. Beer, N.R. *et al.* On-chip, real-time, single-copy polymerase chain reaction in picoliter droplets. *Anal. Chem.* **79**, 8471–8475 (2007).
57. Olsen, M.J. *et al.* Function-based isolation of novel enzymes from a large library. *Nat. Biotechnol.* **18**, 1071–1074 (2000).
58. Aharoni, A. *et al.* High-throughput screening methodology for the directed evolution of glycosyltransferases. *Nat. Methods* **3**, 609–614 (2006).
59. Unger, M.A., Chou, H.P., Thorsen, T., Scherer, A. & Quake, S.R. Monolithic microfabricated valves and pumps by multilayer soft lithography. *Science* **288**, 113–116 (2000).
60. Weinstein, J.A., Jiang, N., White, R.A. III, Fisher, D.S. & Quake, S.R. High-throughput sequencing of the zebrafish antibody repertoire. *Science* **324**, 807–810 (2009).
61. Fan, H.C., Wang, J., Potanina, A. & Quake, S.R. Whole-genome molecular haplotyping of single cells. *Nat. Biotechnol.* **29**, 51–57 (2011).
62. Lecault, V. *et al.* High-throughput analysis of single hematopoietic stem cell proliferation in microfluidic cell culture arrays. *Nat. Methods* **8**, 581–586 (2011).
63. Love, J.C., Ronan, J.L., Grotenbreg, G.M., van der Veen, A.G. & Ploegh, H.L. A microengraving method for rapid selection of single cells producing antigen-specific antibodies. *Nat. Biotechnol.* **24**, 703–707 (2006).
64. Taly, V., Pekin, D., El Abed, A. & Laurent-Puig, P. Detecting biomarkers with microdroplet technology. *Trends Mol. Med.* **18**, 405–416 (2012).
65. Choi, J.W., Kang, D.K., Park, H., deMello, A.J. & Chang, S.I. High-throughput analysis of protein-protein interactions in picoliter-volume droplets using fluorescence polarization. *Anal. Chem.* **84**, 3849–3854 (2012).
66. Joensson, H.N., Zhang, C., Uhlen, M. & Andersson-Svahn, H. A homogeneous assay for protein analysis in droplets by fluorescence polarization. *Electrophoresis* **33**, 436–439 (2012).
67. Srisa-Art, M., Dyson, E.C., Demello, A.J. & Edel, J.B. Monitoring of real-time streptavidin-biotin binding kinetics using droplet microfluidics. *Anal. Chem.* **80**, 7063–7067 (2008).
68. Cecchini, M.P. *et al.* Ultrafast surface enhanced resonance Raman scattering detection in droplet-based microfluidic systems. *Anal. Chem.* **83**, 3076–3081 (2011).
69. Reymond, J.L., Fluxa, V.S. & Maillard, N. Enzyme assays. *Chem. Commun.* **2009**, 34–46 (2009).
70. Joensson, H.N. *et al.* Detection and analysis of low-abundance cell-surface biomarkers using enzymatic amplification in microfluidic droplets. *Angew. Chem. Int. Ed. Engl.* **48**, 2518–2521 (2009).
71. Xia, Y.N. & Whitesides, G.M. Soft lithography. *Angew. Chem. Int. Ed.* **37**, 551–575 (1998).
72. Anna, S.L., Bontoux, N. & Stone, H.A. Formation of dispersions using “flow focusing” in microchannels. *Appl. Phys. Lett.* **82**, 364–366 (2003).
73. Garstecki, P., Fuerstman, M.J., Stone, H.A. & Whitesides, G.M. Formation of droplets and bubbles in a microfluidic T-junction—scaling and mechanism of break-up. *Lab Chip* **6**, 437–446 (2006).
74. Abate, A.R. *et al.* Impact of inlet channel geometry on microfluidic drop formation. *Phys. Rev. E* **80**, 026310 (2009).
75. Sugjura, S., Nakajima, M., Iwamoto, S. & Seki, M. Interfacial tension driven monodispersed droplet formation from microfabricated channel array. *Langmuir* **17**, 5562–5566 (2001).
76. Baret, J.C. Surfactants in droplet-based microfluidics. *Lab Chip* **12**, 422–433 (2012).
77. Baret, J.C., Kleinschmidt, F., El Harrak, A. & Griffiths, A.D. Kinetic aspects of emulsion stabilization by surfactants: a microfluidic analysis. *Langmuir* **25**, 6088–6093 (2009).
78. Roach, L.S., Song, H. & Ismagilov, R.F. Controlling nonspecific protein adsorption in a plug-based microfluidic system by controlling interfacial chemistry using fluorosurfactants. *Anal. Chem.* **77**, 785–796 (2005).
79. Holtze, C. *et al.* Biocompatible surfactants for water-in-fluorocarbon emulsions. *Lab Chip* **8**, 1632–1639 (2008).
80. Chen, F. *et al.* Chemical transfection of cells in picoliter aqueous droplets in fluorocarbon oil. *Anal. Chem.* **83**, 8816–8820 (2011).
81. Hudlicky, M. & Pavlath, A.E. *Chemistry of Organic Fluorine Compounds*. (American Chemical Society, 1995).
82. Skhiri, Y. Dynamics of molecular transport by surfactants in emulsions. *Soft Matter* **8**, 10618–10627 (2012).
83. Woronoff, G. *et al.* New generation of amino coumarin methyl sulfonate-based fluorogenic substrates for amidase assays in droplet-based microfluidic applications. *Anal. Chem.* **83**, 2852–2857 (2011).
84. Courtois, F. *et al.* Controlling the retention of small molecules in emulsion microdroplets for use in cell-based assays. *Anal. Chem.* **81**, 3008–3016 (2009).
85. Siegel, A.C. *et al.* Cofabrication of electromagnets and microfluidic systems in poly(dimethylsiloxane). *Angew. Chem. Int. Ed. Engl.* **45**, 6877–6882 (2006).
86. Asmolv, E.S. The inertial lift on a spherical particle in a plane Poiseuille flow at large channel Reynolds number. *J. Fluid Mech.* **381**, 63–87 (1999).
87. Di Carlo, D., Irimia, D., Tompkins, R.G. & Toner, M. Continuous inertial focusing, ordering, and separation of particles in microchannels. *Proc. Natl. Acad. Sci. USA* **104**, 18892–18897 (2007).
88. Kemna, E.W.M. *et al.* High-yield cell ordering and deterministic cell-in-droplet encapsulation using Dean flow in a curved microchannel. *Lab Chip* **12**, 2881–2887 (2012).
89. Ford, T., Graham, J. & Rickwood, D. Iodixanol—a nonionic isosmotic centrifugation medium for the formation of self-generated gradients. *Anal. Biochem.* **220**, 360–366 (1994).
90. Bruce, A.T. *et al.* Use of iodixanol self-generated density gradients to enrich for viable urothelial cells from nonneurogenic and neurogenic bladder tissue. *Tissue Eng. Part C Methods* **16**, 33–40 (2010).
91. Graziani-Bowering, G.M., Graham, J.M. & Fillion, L.G. A quick, easy and inexpensive method for the isolation of human peripheral blood monocytes. *J. Immunol. Methods* **207**, 157–168 (1997).
92. Burgoyne, F. A remote syringe for cells, beads and particle injection in microfluidic channels. <http://blogs.rsc.org/chipsandtips/2009/08/20/a-remote-syringe-for-cells-beads-and-particle-injection-in-microfluidic-channels/> (20 August 2009).
93. Shapiro, H.M. *Practical Flow Cytometry*. 4th edn. (Wiley-Liss, 2003).
94. Moon, S., Ceyhan, E., Gurkan, U.A. & Demirci, U. Statistical modeling of single target cell encapsulation. *PLoS ONE* **6**, e21580 (2011).
95. Chabert, M. & Viovy, J.L. Microfluidic high-throughput encapsulation and hydrodynamic self-sorting of single cells. *Proc. Natl. Acad. Sci. USA* **105**, 3191–3196 (2008).